Stabilization of fresh and aged simulated pyrolysis oil through mild hydrotreatment using noble metal catalysts

Energy Conversion and Management 313 (2024) 118570

Contents lists available at ScienceDirect

Energy Conversion and Management

journal homepage: www.elsevier.com/locate/enconman

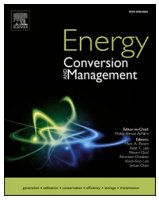

Research Paper

Stabilization of fresh and aged simulated pyrolysis oil through mild hydrotreatment using noble metal catalysts

Elham Nejadmoghadam [a], Abdenour Achour [a], Olov Öhrman [b], Muhammad Abdus Salam [a], Derek Creaser [a], Louise Olsson [a,*]

[a] Chemical Engineering Division, Competence Centre for Catalysis, Chalmers University of Technology, Gothenburg 41296, Sweden
[b] Preem AB, Gothenburg SE-417 26, Sweden

ARTICLE INFO

Keywords:
Simulated pyrolysis oil
Catalytic stabilization
Accelerated aging process
Noble metal catalysts
Coke formation

ABSTRACT

The nature and reactivity of the oxygenates, containing different functional chemical groups, and especially carbonyl compounds, render pyrolysis oil unstable. Alterations in physical and chemical properties of pyrolysis oil during storage and the catalytic stabilization of this oil is therefore critical and is the objective of the current work. In this study, Pd/Al_2O_3, Pt/Al_2O_3, Rh/Al_2O_3, Re/Al_2O_3 and sulphided $NiMo/Al_2O_3$ catalysts were employed in the hydrotreatment (180 °C, 60 bar H_2, 4 h) of simulated pyrolysis oil to examine their effect on stabilization and potential polymerization routes. Of all the catalysts used, Pd/Al_2O_3 with well-dispersed metal particles, and a high char-suppressing potential was the most effective catalyst. It had the highest bio-liquid yield and the highest selectivity to low molecular weight stabilized oxygenates and deoxygenated products. In addition, the acidity in the light fraction was low and a very low solid product formation was found that consisted mainly of soluble polymers composed predominantly of aliphatic compounds and sugars, whereas insoluble polymers were not fully developed char. The solid yield increased in the following order: Pd (3.3 wt%) < Rh (13.3 wt%) < NiMo (13.6 wt%) < Pt (21.5 wt%) < Re (25.8 wt%) < Blank (27.4 wt%). This trend was also accompanied by an enhanced yield of heavy oligomers in the corresponding liquid phase abundant in phenolic compounds compared to carboxylic acids and aliphatic compounds based on GPC and P-NMR analyses. The Pd loading necessary to obtain a high-quality product was also assessed, and the lower carbon loss when using catalysts with smaller contents of metal was revealed. Based on the results a detailed reaction network was proposed regarding the reactions during stabilization of sugars, aldehydes, ketones, furans, acids and phenols present in pyrolysis oil. To delve deeper into the simulated pyrolysis oil properties, it was subjected to accelerated aging. Interestingly as much as 79 % of the feed was converted during aging. According to GC/MS analysis only large oligomers were formed that could not be detected. When removing the most reactive components from the feed, i.e. the sugar and furan, the conversion was lowered to 53 %. Catalytic stabilization was conducted on the aged oil and compared with stabilization followed by aging. The results showed that the solid formation increased from 5.1 to 9.1 % when the pyrolysis oil was first aged, followed by stabilization. A suggested reason for this is the large amount of oligomers that were formed during the aging. Thus, aging before stabilization is very negative for an industrial process.

1. Introduction

Fast pyrolysis is a promising method for the direct thermochemical production of bio liquids from biomass with a great potential for renewable fuel production [1–6]. Pyrolysis oils are produced by heating the biomass rapidly to temperatures of 450–550 °C in the absence of oxygen. They are characterized by a high water concentration and comprise a complicated blend of oxygenated organic compounds, resulting in non-miscibility with petroleum, high reactivity, and thus chemical instability [7]. There is ongoing concern regarding the aging of pyrolysis oil during storage, and its potential impact on performance and its quality due to viscosity and compositional changes [8]. Over time, pyrolysis oil undergoes aging processes at room temperature, characterized by chemical degradation, polymerization, and oxidation

* Corresponding author.
E-mail address: louise.olsson@chalmers.se (L. Olsson).

https://doi.org/10.1016/j.enconman.2024.118570
Received 11 February 2024; Received in revised form 14 May 2024; Accepted 16 May 2024
Available online 31 May 2024

reactions, which adversely affect its quality. The inherent properties of pyrolysis oil therefore require it to be upgraded prior to being used as an alternative fuel [9]. This can be achieved via deoxygenation at high temperatures (>300 °C), with high hydrogen pressure and the presence of a heterogeneous catalyst, which is known as hydrodeoxygenation (HDO) [10–19]. However, direct HDO under severe conditions is usually problematic due to the condensation reactions associated with high temperatures that leads to a significant charring of the pyrolysis oil. Direct HDO can therefore result in a decline in catalytic activity mainly because of coking of the catalyst and also a large carbon loss due to coke and char formation. To overcome these limitations, a two-step process has received considerable attention [12,16,17,20–22]. The first step is intended to stabilize the most reactive compounds by catalytic hydroprocessing under mild conditions. Subsequently, the stabilized bio-oils are further processed using HDO at higher temperature and pressure to selectively eliminate oxygen atoms and increase the bio-oil quality.

Alongside the benefits of catalytic stabilization, understanding the intricate aging mechanisms of pyrolysis oil during storage is paramount. Accelerated aging process is a well-known method that has been used in several studies to assess the stability of pyrolysis oil [8,23–25]. The most commonly used accelerated aging protocol involves a 24 h heat treatment of pyrolysis oil at 80 °C corresponding to a natural aging of 6–12 months of storage at room temperature. However, findings from a prior investigation by the National Renewable Energy Laboratory (NREL) group [24] suggest that this condition is too harsh to accurately simulate aging at room temperature and thus accelerated aging for 2 h at 80 °C was proposed. In another study by Wang *et al.* [25], the aging behaviour of different model compounds were evaluated at 80 °C for 72 h to investigate the aging mechanism. Acids were identified as significant contributors affecting the aging process of pyrolysis oil due to their dual role as both reactants and catalysts. Notably, they did not assess a mixture containing all main compounds present in pyrolysis oil in their study, only binary mixtures such as compounds in the groups of sugars and acids, furans and acids, aldehydes and ketones, as well as furans and phenols.

Stabilization of pyrolysis oil using various noble metals has been studied at mild conditions [26,27]. Payormhorm *et al.* [26] studied the effect of a noble metal on upgrading of bio-oil obtained from pyrolysis of Leucaena leucocephala at mild conditions (300 °C, 2 bar N_2, 1 h). They proposed that Pt/Al_2O_3-catalytic deoxygenation successfully reduced the oxygenated compounds in the pyrolysis oil from O/C molar ratio of 0.43 to 0.18 via C-O bond cleavage to form hydrocarbons and water after deoxygenation [26]. In another study [27], the performance of NiMo/Al_2O_3 and Ru/Al_2O_3 catalysts for the stabilization of pyrolysis oil at 250 °C, 100 bar hydrogen was evaluated. The NiMo/Al_2O_3 catalyst was superior compared to Ru/Al_2O_3 in terms of the yield of oil produced (31 wt% compared to 24 wt% when using Ru), and deoxygenation level of 0.31O/C molar ratio for NiMo/Al_2O_3 compared to 0.38 for Ru/Al_2O_3 [27].

Single model compounds are studied significantly for many reasons, but the primary one is to study the structure and reactivity of specific oxygenated functional groups [12,28–35]. In the literature, guaiacol has been examined as a lignin monomer to study its conversion and product quality during mild hydrotreatment using different noble metal catalysts [28,29]. Lee *et al.* [28] concluded that among SiO_2-Al_2O_3 supported Pd, Rh, Ru and Pt, guaiacol was completely converted in the presence of Rh and Ru, with the highest selectivity being towards hydrogenation of aromatic rings followed by deoxygenation yielding cyclohexane at 250 °C. In another study by He *et al.* [29], NiMo/Al_2O_3 had a better performance than Pt/Al_2O_3 at 285 °C and 4 MPa hydrogen for guaiacol conversion, with higher activity and selectivity towards cyclohexane by ring hydrogenation along with a reduced formation of coke. Hydrodeoxygenation occurred due to a synergy effect, where hydrogen molecules dissociated on metal sites and dehydration of cyclohexanol to cyclohexene occurred on the acid sites of Al_2O_3 [29]. A similar observation was reported in the case of mild hydrotreatment of m-cresol in the presence of Pt/Al_2O_3 at 300 °C and atmospheric pressure, where a low coke yield was found and a high selectivity to produce toluene via either dehydration on the acid sites or hydrodeoxygenation on the Pt sites [33]. Evaluation of mild catalytic hydrotreatment of a cyclic ketone (cyclohexanone) [30] at 300 °C using Pt/Al_2O_3 indicated significant dehydrogenation to phenol as the dominant product with a selectivity up to 90 %. Although, condensation reactions also occurred simultaneously, it resulted in a low yield of coke [30]. Bhogeswararao *et al.* [31] also reported that using Pt/Al_2O_3, selective hydrogenation of the carbonyl bond in furfural plays a vital role in its ability for ring-opening whilst use of a Pd/Al_2O_3 catalyst facilitates hydrogenation of the furan ring, with excellent decarbonylation activity at 240 °C. A catalyst screening was performed [32] on a pool of non-furanic carbonyl groups, comprising acetaldehyde, propanal, acetone and xylose and furanic compounds such as furfuryl alcohol, and tetrahydrofurfuryl alcohol (THFA) in the presence of various noble metal catalysts (alumina-supported Ru, Pd, Pt, and Rh) and Ni/Al_2O_3. Ru/Al_2O_3 (3 wt%) exhibited the best performance for the hydrogenation of non-furanic carbonyl groups. However, polymerisation was the dominant reaction in the catalytic hydrotreatment of the furan THFA using Ru, which led to severe coking. Oppositely, the Pd was the most active metal for hydrogenation of carbonyl groups attached to the furan rings. The Pd/Al_2O_3 catalyst revealed the highest initial rates for hydrotreatment of the furanic carbonyl group in furfural (0.128 s^{-1}) and the C = C bond in furfuryl alcohol (0.076 s^{-1}). The reduction in the initial activity for hydrotreatment of furfural was reported to follow: Pd~Ni > Ru > Pt > Rh.

Based on the above-mentioned studies on single model compounds and real pyrolysis oils, it is beneficial to design a simulated mixture to simplify the complex composition of real pyrolysis oil, as well as to provide an opportunity to elaborate on the behaviour of different oxygenated groups present simultaneously in such oils. There are some studies available that have examined different model compounds together [36–43]. For example, acids and phenols were studied by Wan *et al.* [36], who reported hydrotreatment of a mixture of acetic acid and p-cresol to simulate pyrolysis oil over a Ru/C catalyst at mild conditions of 300 °C and 48 bar H_2. They found that hydrogenation of acetic acid was suppressed by p-cresol, whereas p-cresol HDO was favoured in the presence of acetic acid [36]. Chen *et al.* [37] studied the stabilization of a simulated pyrolysis oil containing acetic acid, guaiacol, phenol, furfural and hydroxyacetone over Pt-Fe, Pt-Ni, Pd-Fe, and Pd-Ni catalysts supported on SiO_2 at 240–300 °C, using ethanol as an H-donor. They found that Pt-Fe/SiO_2 and Pt-Ni/SiO_2 were the best catalysts in terms of conversion of acid-rich pyrolysis oil and the hydrogenation of pyrolysis oil rich in phenols, respectively [37]. The coke yield ranged from 1.1 to 1.9 wt%, whereas no information was reported regarding its composition. In another study the mixture of hydroxyacetone, furfural, and phenol was studied by Han *et al.* [38] to evaluate the effect of interactions among model compounds on their conversions during mild hydrotreatment using Ni/SiO_2, at 180 °C and 3.5 MPa H_2. They observed the inhibitory effect of furfural on the conversions of hydroxyacetone and phenol along with a strong inhibitory effect of furfural on hydroxyacetone compared to corresponding experiments using single model compounds. Boscagli *et al.* [39] investigated the mild catalytic hydrotreatment of a light fraction of straw pyrolysis oil composed of sugar derivatives, phenol derivatives, furans, acids, aldehydes, ketones, and alcohols at 250 °C and 8 MPa hydrogen pressure. Performance of various nickel-based catalysts such as NiCu/Al_2O_3, Ni/ZrO_2, Ni/SiO_2, Ni/TiO_2, Ni/Al_2O_3 were compared with a Ru/C catalyst at identical reaction conditions. While the nickel-based catalysts exhibited a slightly greater level of deoxygenation with NiCu/Al_2O_3 being most effective, Ru/C yielded an upgraded oil with a higher degree of hydrogenation. In another study [40] a Ni/CMK-3 catalyst was applied for stabilization of an oxygenated mixture (acetone, acetic acid, furfural, o-cresol, ethanediol, and water) using various solvents as hydrogen donors comprising methanol, ethanol, and formic acid at a temperature of 230 °C, without adding external hydrogen. The study revealed that the choice of solvent had an

impact on both the conversion of model compounds and the reaction progression and thus product selectivity. It was found that interactions like esterification took place between acetic acid and the alcohol-based hydrogen donors. Also, when formic acid was used, the phenol conversion showed an increase exceeding threefold, but the conversion of acetic acid was reduced to one fifth. In another study [41] mild hydrotreatment of phenolic compounds separated from bio-oil by a modified glycerol-assisted distillation technology, to alcohols using a Ru/SBA-15 catalyst at 120 °C was evaluated. Their main observations were the effective conversion of phenolic compounds along with no catalyst deactivation during stabilization of such a simulated pyrolysis oil. However, the process was not stable when using real pyrolysis oil. Other hybrid model compounds (acetic acid, furfural, hydroxyacetone, ethanediol, phenol and water) were chosen by Ying *et al.* [42] for stabilization into esters and alcohols using Raney Ni catalysts (RN) and Mo, Sn, Fe, Cu modified Raney Ni catalysts (RNs) at 180 °C, 5 Mpa H_2 in the presence of methanol and the liquid product distribution was documented. Among the various RNs, 100 % conversions of hydroxyacetone and furfural were obtained, and Mo-RN exhibited the most favourable performance in the hydrogenation of phenol, while Fe-RN demonstrated remarkable suppression of alkylation reactions. In our previous study [43], a mixture, containing acetic acid, levoglucosan, benzaldehyde, HMF, hydroxyacetone, and guaiacol, was comprehensively investigated using a conventional $NiMo/Al_2O_3$ catalyst at 180 °C, 60 bar H_2 during 4 h reaction. According to our observations [43], among different oxygenates present in the feed mixture, sugars and furans were found to easily condensate and form a solid/char-like material. Furthermore, cross-linking of these two reactive oxygenates with other intermediates and even each other was reported as creating an initiator in the formation of heavy oligomer precursors and, consequently, solids [43]. Similarly, cross-polymerization between furans and phenols as well as furans and sugars during thermal treatment of pyrolysis oil were reported respectively in previous works [44–46].

Thus, both noble metals and non-noble metal catalysts have been examined for pyrolysis oil upgrading. Non-noble transition metal catalysts offer cost advantages, since noble metals inevitably have a high feedstock price. However, as pointed out in a comprehensive literature review [47], the requirement for more frequent active phase reactivation for non-noble metal catalysts undermines the initial cost benefits of cheaper materials. Also, the noble metal catalysts can be used in sulphur free conditions when upgrading 100 % green feedstock, which is an advantage. Thus, despite the initial higher cost, noble metal catalysts, with their prolonged lifetime, and hydrogenation capacity (even under mild operating conditions) [5,48–50] with lower metal loadings up to 10 times less than transition metal sulfide catalysts, may present an economically and operationally possible alternative. Furthermore, several studies reported the effectiveness of noble metal catalysts maintaining their activity over multiple utilization – regeneration cycles during the hydrotreatment of pyrolysis oils or their model compounds [33,51–54]. A study by Xu *et al.* [51] demonstrated that Pd supported on mesoporous N-doped carbon retained its catalytic activity for mild hydrotreatment of vanillin even after six cycles without any loss of activity. Similarly, Tran *et al.* [52] investigated the HDO of guaiacol using an Al-MCM-41 supported Pd–Fe catalyst, which showed regeneration capability and consistent activity over three HDO cycles. In another study [33], the catalytic activity of Pt/Al_2O_3 catalyst for HDO of m-cresol was recovered in a new reaction cycle through regeneration in H_2 at 450 °C and 0.5 atm. The effectiveness of Pt/Al_2O_3, Pt/SiO_2, and Pt/Na-B catalysts after regeneration was also assessed for m-cresol HDO [53]. The recovered catalysts exhibited equivalent activity and selectivity towards toluene in the second cycle, similar to the first cycle. Another study evaluated the regeneration performance of ZrO_2-supported Rh catalyst for the hydrogenation of guaiacol [54], achieving a conversion rate of 92.4 mol% with the regenerated catalyst.

Despite the studies mentioned regarding stabilization of pyrolysis oil and different model compounds, there are still many unanswered questions regarding stabilization of pyrolysis oil and its mechanistic aspects. This study delves into a comprehensive examination of the pyrolysis oil's behaviour during catalytic mild hydrotreatment, aiming to enhance understanding of stabilized oil composition and solid/char formation in the stabilization process. Due to the complex nature of real pyrolysis oil, we examined catalytic stabilization using a complex simulated pyrolysis oil mixture, including the important functional groups, i.e. phenols, furans, sugars, acids, aldehydes, and ketones present in real pyrolysis oil. The selection of feed compounds was based on their abundance in the corresponding oxygenated groups in pyrolysis oil derived from lignocellulosic biomass found in the literature [16,55–58]. In more detail, we have studied catalytic stabilization of a mixture containing guaiacol, HMF, levoglucosan, acetic acid, benzaldehyde, and hydroxyacetone as representative compounds from different oxygenated groups. The effect of noble metal catalysts composition for the stabilization of simulated pyrolysis oil, and its char-suppressing potential are studied in detail using Pd/Al_2O_3, Pt/Al_2O_3, Rh/Al_2O_3, Re/Al_2O_3 and are compared with sulphided $NiMo/Al_2O_3$. In this work, we have for the first time according to our knowledge examined the effect of stabilization of pyrolysis oil after it underwent a rapid aging treatment. We found the aging to be detrimental for the stabilization process resulting in significantly more solid formation. Interestingly, we could also show that when using our most efficient catalyst (Pd/Al_2O_3) and stabilizing the oil prior to aging, less solids were formed. Aging studies after pyrolysis oil stabilization has according to our knowledge not been previously studied.

2. Experimental

2.1. Preparation of the catalysts

All catalysts were prepared by incipient wetness impregnation, using metal salt solutions (NH_4ReO_4, $Rh(NO_3)_3$, $N_4O_{12}Pt$, $Rh(NO_3)_3$, and $Pd(NH_3)_4(NO_3)_2$). $NiMo/Al_2O_3$ catalyst preparation has been reported in our previous study [43]. ϒ-alumina support was initially calcined at 550 °C for 8 h according to our previous work. After the metal impregnation, the catalysts were dried at 60 °C (12 h) and then at 110 °C (12 h), followed by calcination at 550 °C using a heating rate of 2 °C/min (12 h). One day prior to performing the catalytic hydrotreatment experiments, catalysts pre-treatments were carried out, where all calcined noble metals and Re catalysts were reduced at 300 °C and 15 bar hydrogen for 4 h in a Parr autoclave reactor (450 ml). The samples were cooled down to room temperature and then passivated under a flow of 2 % O_2/N_2 at 25 ml min^{-1} for 1 h before being exposed to air. However, in the case of $NiMo/Al_2O_3$, sulphidation was done to obtain its sulphided state using 2000 μl dimethyl disulphide (DMDS) added to 1 g catalyst at 340 °C and 20 bar hydrogen for 4 h. Thereafter the sample was passivated using the same procedure above. Catalyst characterization techniques and materials used are detailed in Supplementary Information (SI) in Sections S1 and S2.

2.2. Catalytic stabilization of simulated pyrolysis oil

The performance of various noble metals and conventional $NiMo/Al_2O_3$ catalysts for stabilization of simulated pyrolysis oil, as well as the effect of an aging process on simulated pyrolysis oil, were evaluated in a 450 ml stainless steel Parr reactor. The simulated pyrolysis oil consisted of the following six compounds: acetic acid, levoglucosan, benzaldehyde, HMF, hydroxyacetone, and guaiacol. Also, another mixture containing acetic acid, benzaldehyde, hydroxyacetone, and guaiacol (1 g of each compound, along with appropriate amount of hexadecane as a solvent to maintain the total feedstock amount consistent with the previous sample) was subjected to the aging test. This involved heating the two feedstock samples at 80 °C for 2 h under a nitrogen flow in the Parr reactor. Subsequently, aged oil obtained from the mixture of 6 model compounds underwent stabilization in the presence of Pd/Al_2O_3.

The aged samples were denoted *Aged feed 6* and *Aged feed 4*, for the two aged oils, respectively. A detailed description of the reactor experiments is given in our previous work [43]. In brief, experiments using the simulated pyrolysis oil mixture (1 g of each compound, resulting in 6 g in total), with hexadecane as a solvent (150 ml), and pre-sulphided NiMo/Al_2O_3 and reduced noble metal catalysts (1 g) were performed. It should be noted that, a mixture of six compounds (Figure S1), each in equal amounts, was shrewdly selected to enable comparison of different organic groups under identical conditions and indeed control and standardize the composition, which can be difficult to achieve with real pyrolysis oil due to variations in biomass feedstock and pyrolysis conditions. For NiMo/Al_2O_3, DMDS (166 μl) was added to keep the catalyst in a sulphided state during the reactor experiment. Then, the reactor was heated up to 180 °C, at an average heating rate of 12 °C/min. The reaction was conducted at this temperature using 60 bar H_2 for 4 h. A blank experiment without catalyst was also conducted using the same reaction conditions. After the reaction, the reactor vessel containing liquid, and solid products along with catalyst (1 g) was weighed and compared with empty vessel and vessel containing simulated pyrolysis oil solution masses. The residual difference from this comparison from experiments using various catalysts, was only about 1.1–1.8 wt%. Accordingly, any losses and/or gas formation were minor and were therefore neglected. The procedure for collecting liquid and solid products and their characterization is depicted in Figure S1. Multiple analytical techniques, such as gas chromatography-mass spectroscopy (GC–MS), volumetric Karl Fisher titration, two dimensional heteronuclear single-quantum coherence (HSQC)-NMR, 31-P nuclear magnetic resonance (P-NMR), gel permeation chromatography (GPC) and CHOS elemental analysis were used to analyze the product phases from the mild hydrotreatment process. Section S3 in Supplementary Information contains detailed descriptions. For the extraction methods employed for liquid and solid products, we refer to Section S4.

3. Results and discussion

3.1. Characterization of the catalysts

The composition and catalytic properties of various metal supported-alumina catalysts were characterized by ICP-SFMS, BET and XRD to elucidate their surface properties. The metal loadings, determined using ICP-SFMS (see Table 1), are 1.8, 1.7, 1.8, and 1.9 respectively corresponding to Pd, Pt, Rh, and Re, whereas for the NiMo/Al_2O_3 catalyst the loading was 13.2 wt% Mo and 3.6 wt% Ni. The N_2 adsorption–desorption isotherms and pore size distribution of the support and catalysts are also reported in Table 1. All samples display a typical type V hysteresis loop (Figure S2, Section S5, Supplementary information) according to the BET classification, which is characteristic of mesoporous materials. Upon addition of metal on the alumina support (192.3 m^2g^{-1}), the BET surface areas only slightly decreased (181.4 – 191.0 m^2g^{-1}) for the catalysts with low metal loadings (monometallic). However, for NiMo/Al_2O_3, as can be seen in Table 1, the surface area and pore volume decreased were much more pronounced, due to the significantly higher loading of metals compared to the monometallic catalysts.

Table 1
Textural properties of the catalysts examined, and their loadings determined by ICP-SFMS analysis.

Samples	S_{BET} [a] (m^2/g)	V_p [b] (cm^3/g)	Average particle size [c] (nm)	Metal loading [d] (wt%)		Sample notations
ϒ-Al_2O_3	192.3	0.48	–	–		–
Pd/ϒ-Al_2O_3	181.4	0.46	4.4	1.8		Pd-1.8
Pt/ϒ-Al_2O_3	183.6	0.46	16.0	1.7		Pt-1.7
Rh/ϒ-Al_2O_3	182.2	0.45	1.9	1.8		Rh-1.8
Re/ϒ-Al_2O_3	183.4	0.46	3.1	1.9		Re-1.9
NiMo/ϒ-Al_2O_3	137.4	0.33	1.0 (μm)	Ni Mo	3.6 13.2	NiMo-3.6,13.2

[a] Calculated by the BET method.
[b] Pore volume.
[c] Determined by TEM.
[d] Metal loadings determined by ICP-SFMS.

The XRD patterns of the bare support along with reduced Pt/Al_2O_3, Rh/Al_2O_3, Re/Al_2O_3, and Pd/Al_2O_3 as well as sulphided NiMo/Al_2O_3 catalysts are shown in Fig. 1. As shown, all the catalysts exhibited the characteristic XRD peaks of ϒ-Al_2O_3 around 2θ of 37, 39, 46 and 67° [59,60]. No peaks attributed to Re and Rh can be detected for Re/Al_2O_3 and Rh/Al_2O_3 catalysts. The reason for this could be that either the loading of Re and Rh was too low or that they were well dispersed, resulting in that they could not be detected by XRD. Pt exhibited two characteristic peaks that could correspond to the (111) and (311) planes at 40.5 and 82°, respectively, analogous to the positions found for Pt on Pt/Al_2O_3 catalyst at 39.5 and 82° by Garidzirai *et al.* [61]. A small peak at 34° was detected for the Pd/Al_2O_3 catalyst, which is associated with PdO [62]. In the case of the bimetallic NiMo/Al_2O_3, XRD analysis confirmed two peaks at 23.5° and 26.7°, which correspond to the MoO_3 phase; no relevant peak for Ni was seen, presumably due to its good dispersion or loading below the detection limit of the XRD [59].

The catalysts were further characterized by SEM and TEM to determine the surface morphology and particle size distribution (Figure S3, SI). The average metal particle sizes, which are of paramount importance to boost catalyst activity, are also determined and listed in Table 1. It is clear from the results that Pt/Al_2O_3 exhibited a poor dispersion with particle size on average 16 nm. However, the other noble metal catalysts exhibited more similar particle sizes ranging from 1.9 nm for Rh/Al_2O_3 to 4.4 nm for Pd/Al_2O_3. In the case of the sulphided NiMo/Al_2O_3 catalyst, it had an apparent flower-like morphology with higher number of particles on the catalyst surface with sizes ranging from 0.1 to 2.0 μm thanks to the higher metal loadings. Also, its TEM micrograph showed typical structures of the NiMoS and MoS_2 phases [63]. The black thread-shape fringes indicate dispersion of MoS_2 slabs on the surface of alumina with an interlayer distance of 0.62 nm relating to the (002) basal planes of MoS_2.

3.2. The effect of catalyst composition on the stabilization process

3.2.1. Conversions and product yields

The mild hydrotreatment of simulated pyrolysis oil using various catalysts was studied at 180 °C, 60 bar H_2 and 4 h with the aim of stabilizing the reactive intermediates/products. The amount of different fractions, e.g. liquid and solid products, water and unreacted simulated pyrolysis oil obtained in different experiments were calculated to determine the overall mass balance. Fig. 2 shows the conversion and product distributions obtained using Pt/Al_2O_3, Rh/Al_2O_3, Pd/Al_2O_3 and Re/Al_2O_3 as well as the conventional sulphided NiMo/Al_2O_3. A blank experiment under the same reaction conditions, but without a catalyst, was conducted for comparison (Fig. 2f). In all experiments, including the blank, the conversion reached approx. 100 % for HMF, levoglucosan and hydroxacetone, whereas the conversion of other oxygenates in the feedstock (acetic acid, benzaldehyde and guaiacol) varied. The conversion of acetic acid was about 80 % in the presence of Pt/Al_2O_3, Pd/Al_2O_3 and Rh/Al_2O_3 catalysts, but slightly below 80 % for the other catalysts, Re/Al_2O_3, NiMo/Al_2O_3 as well as the blank experiment. The highest conversion of benzaldehyde (~70 %) was obtained by Pd/Al_2O_3 and for Pt/Al_2O_3 and Rh/Al_2O_3 catalysts the conversion was about 40 %; however, in the presence of Re/Al_2O_3, NiMo/Al_2O_3 and absence of catalyst, it was below 40 % and showed its lowest conversion in the blank experiment (below 20 %). Apart from benzaldehyde, guaiacol conversion also showed noticeable variations with and without different

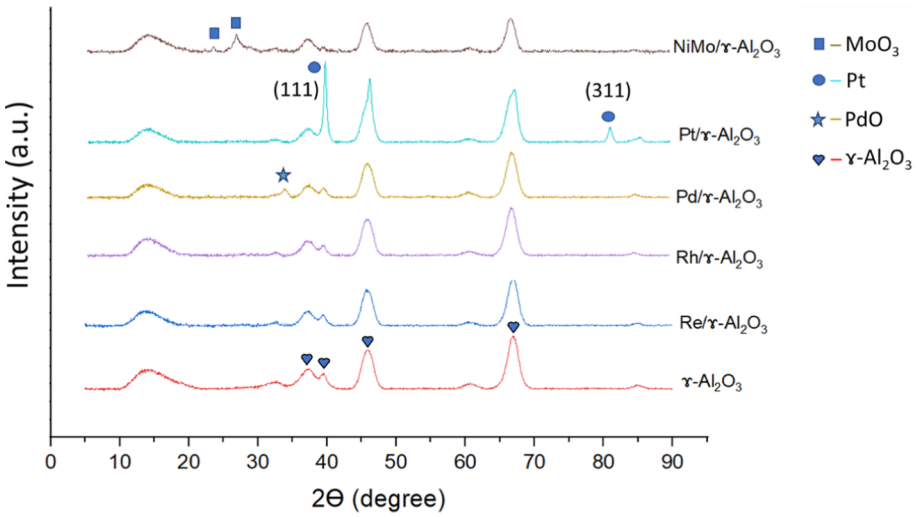

Fig. 1. XRD patterns of the catalysts employed.

catalysts. Contrary to benzaldehyde conversion, minimum conversion of guaiacol was exhibited when using the $NiMo/Al_2O_3$, Pt/Al_2O_3, and Rh/Al_2O_3 catalysts, reaching about 20 %, although its conversion was enhanced to about 30 % when using the other examined catalysts (Re/Al_2O_3, Pd/Al_2O_3) and for the blank experiment. Overall, the highest yield of converted/reacted simulated pyrolysis oil was obtained in the presence of Pd/Al_2O_3 (81.6 wt%, according to Fig. 2).

In Fig. 2, the effect of catalysts on yields of liquid product was also shown. As can be seen, the liquid product yields (determined from mass balances) decreased from 65.9 wt% to 26 wt% in the following catalytic order: Pd/Al_2O_3 (65.9 wt%) > Rh/Al_2O_3 (51.2 wt%) > Pt/Al_2O_3 (48.5 wt%) > $NiMo/Al_2O_3$ (42.1 wt%) > blank (41.7 wt%) > Re/Al_2O_3 (31.7 wt%). Re/Al_2O_3 gave a considerably lower liquid yield of 31.7 wt%. Surprisingly, this yield is even lower than the corresponding yield of 33.1 wt% for the blank experiment. These results could be explained by the high solid yield for Re/Al_2O_3, suggesting that Re/Al_2O_3 catalyses further repolymerization to form solids compared to the other tested catalysts. As depicted in Fig. 2, the liquid product obtained from all experiments encompasses the light compounds and heavy oligomers (determined from mass balance) produced during mild hydrotreatment, namely GC detectable molecules and undetectable heavy oligomers, respectively. The highest yields of light compounds in the liquid product were obtained when applying Pd/Al_2O_3, Rh/Al_2O_3 and $NiMo/Al_2O_3$, which can be attributed to lower rates of condensation and oligomerization reactions with these catalysts. This result correlates well with their corresponding low solid yields obtained under these mild conditions. However, with other catalysts, particularly for Re, the liquid product was largely comprised of heavy oligomers, as was also the case for the blank experiment, where 84 % of the liquid was heavy oligomers.

The measured water yields from stabilization of the simulated pyrolysis oil using various catalysts were in the range of 3.9 to 12.4 wt%. Produced water is likely mainly caused by hydrodeoxygenation (HDO) reactions [64,65]. The occurrence of water formation via subsequent reactions of intermediate alcohols to produce esters, and ethers [66,67] and production of deoxygenated compounds accompanied by water formation [65] will be discussed in detail in the next Section. The Pd/Al_2O_3 catalyst exhibited the highest water yield of 12.4 wt% indicating the promoting effect of this catalyst for hydrodeoxygenation reaction at these mild conditions. Indeed, this catalyst also exhibited the highest overall liquid yield as well as the highest amount of GC detectable compounds. Whilst in other catalytic and blank experiments, the water yields decreased to 10.7, 7.1, and 6.9 wt% for $NiMo/Al_2O_3$, Re/Al_2O_3, Rh/Al_2O_3 respectively, and reached the lowest yield of 3.9 wt% for Pt/Al_2O_3. Oh *et al.* observed higher water content in the presence of Ru compared to Pt during mild hydrotreatment of pyrolysis oil [68].

Along with the formation of water and liquid products, solid products were also formed not only in the absence of a catalyst but also in the presence of all examined catalysts, similar to observations in previous works [27,69]. As expected, the solid yield was high without catalyst and indeed the solid formation was lower for all studied catalysts. In addition, Re/Al_2O_3 exhibited large solid formation, however not as high as the blank experiment. These findings are in line with the results that the Re/Al_2O_3 and blank experiments had high levels of large oligomers (GC undetectable) in their formed liquids (see Fig. 2). The behaviour of each catalyst is elaborated upon in Section 3.2.1 by tracking the degree of hydrogenation and condensation reactions via GC/MS analysis.

3.2.2. *Liquid product distribution*

The composition of liquid yields produced from thermal and catalytic hydrotreatment were quantitively identified by using GC/MS. The functional groups were commonly found, and products accordingly categorized as phenolics, carboxylic acids, ketones, aldehydes, alcohols, furan derivatives, esters, ethers, hydrocarbons (oxygen-free compounds) as well as other types of multi-oxygenated compounds that mainly consisted of sugars, furans, and aldehyde derivatives. The composition of light liquid products obtained from the blank experiment, Re/Al_2O_3, noble metals and $NiMo/Al_2O_3$ catalysts are displayed in Fig. 3. In Fig. 3a, the Re/Al_2O_3 catalyst exhibited the lowest GC detectable composition of 4.9 wt% yield, which mainly consists of multi-oxygenated compounds. This result is comparable to the blank experiment (Fig. 3e) that also yielded a small amount of GC detectables (5.4 wt %). Moreover, it can be observed that the yields of other oxygenated monomers (furans, ethers, and esters) were significantly lower for the Re catalyst (Fig. 3a) along with a high yield of alcohol, but no phenols, ketones, acids, and oxygen free compounds were detected.

In our previous work [43], the experiments revealed that furans and sugars were the reactants that caused the largest formation of solids which may due to their high reactivity and cross-polymerisation tendency. In the blank experiment (Fig. 3e), very small amounts of furans are detected in the products, suggesting that the furan type of compounds underwent polymerization reactions forming large amounts of oligomers [44,70], and humin [71–73], with opening of furan rings [44,70], and consequently solid formation. Therefore, low yields of furans ($\leq$0.5 wt%) were also obtained when using Re/Al_2O_3, along with its high solid yield indicating the poor performance of this catalyst on stabilizing this reactive oxygenated group and as a result compared to other catalysts, higher degrees of irreversible condensation and polymerization occurred. This explanation agrees with condensates being

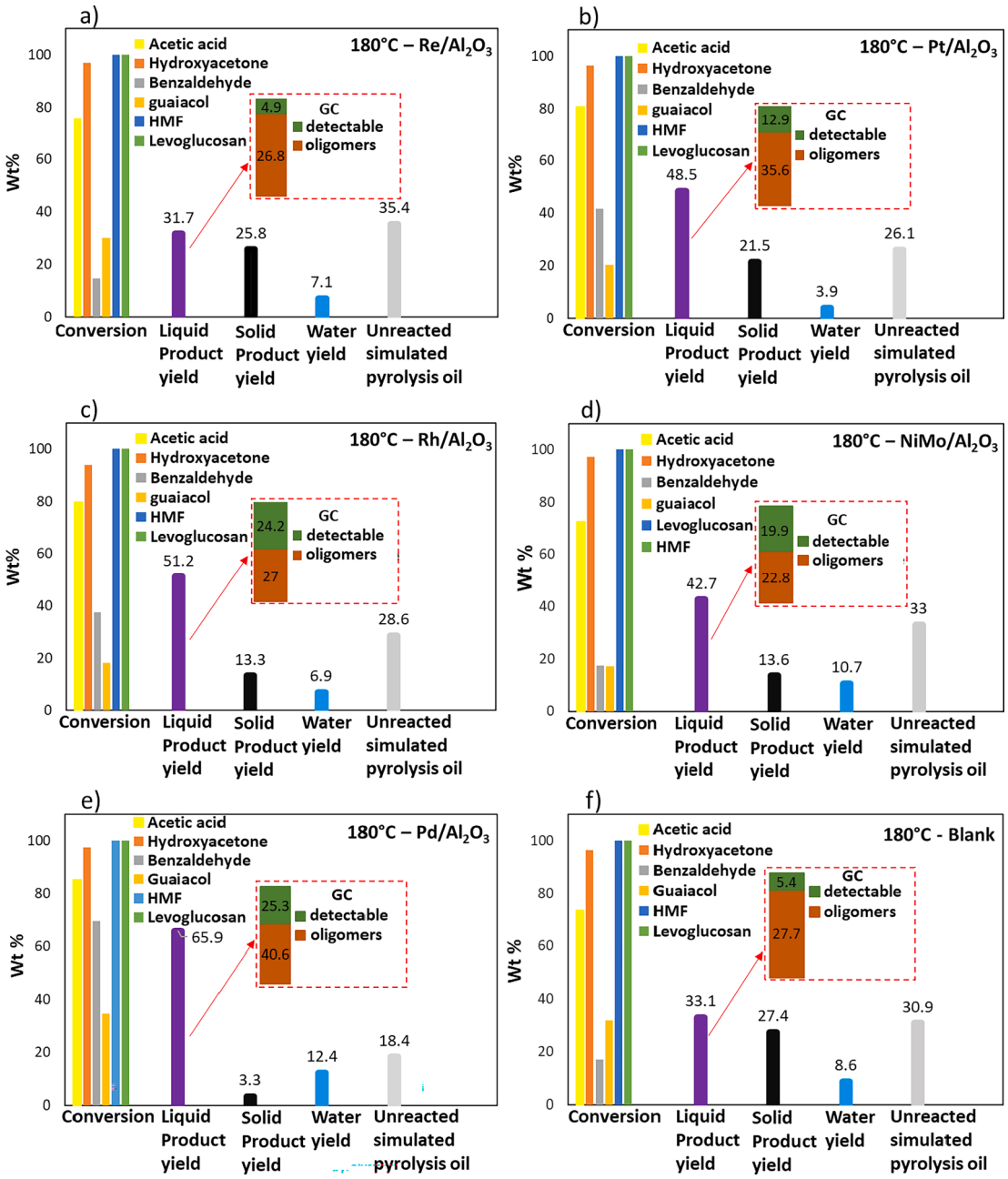

Fig. 2. Conversion of oxygenated compounds in simulated pyrolysis oil, and yields of liquid and solid products, water, and unreacted simulated pyrolysis oil (wt%) over 1 g alumina supported a) Re, b) Pt, c) Rh, d) NiMo, e) Pd catalysts and f) blank experiment. Reaction conditions: 180 °C and 60 bar H_2 for 4 h. The yields of oligomers are determined from mass balance.

formed and depicted as multiple oxygen group compounds from furans and sugars (Fig. 3a). Therefore, in the case of Re/Al_2O_3, similar to the blank experiment, it seems that reactions of the furans and sugars play an important role in polymerisation reactions and thereby solid content.

The Pt/Al_2O_3 catalyst (Fig. 3d), on the other hand, exhibited better performance compared to Re/Al_2O_3 in terms of the yield of the light liquid fraction (12.9 wt%) and different oxygenates, particularly multiple oxygen groups (6 wt%), alcohols (4 wt%) and furans (2 wt%). However, no oxygen free compounds, phenols, acids, and ketones were observed, and the yield of multi-oxygenated compounds composed of condensed compounds from sugars, furans, and aromatics, was higher. The Pt/Al_2O_3 was to a higher degree able to stabilize the furanic compounds in the light liquid fraction and thereby lowered the polymerization and solid formation compared to Re/Al_2O_3 (Fig. 2). Moreover, the high conversion of acetic acid (Fig. 2) and the absence of acid products obtained from GC using Pt/Al_2O_3, is in line with observations by French *et al.* [74].

Regarding the Rh/Al_2O_3 and $NiMo/Al_2O_3$ (Fig. 3b, and 3e), compared to previously mentioned catalysts, the amount of GC detectable compounds significantly increased, and in addition their compositions changed with higher yields of alcohols, esters, and furans such as 2,5-dimethylfuran (DMF). These results are in line with the report by French *et al.* [74] regarding the high effectivity of NiMo-S/Al_2O_3 for deoxygenation. Comparing $NiMo/Al_2O_3$ and Rh/Al_2O_3 (Fig. 3b, and 3e), the distributions of light liquid product were different whereas the yields of their solid products were almost same (Fig. 2). In the case of $NiMo/Al_2O_3$, a higher yield of oxygen free compounds, ketones and furans and a lower yield of alcohols and esters were obtained. This demonstrates that hydrodeoxygenation was promoted in the presence of the $NiMo/Al_2O_3$ catalyst, as it is well-known that traditional sulphided NiMo/

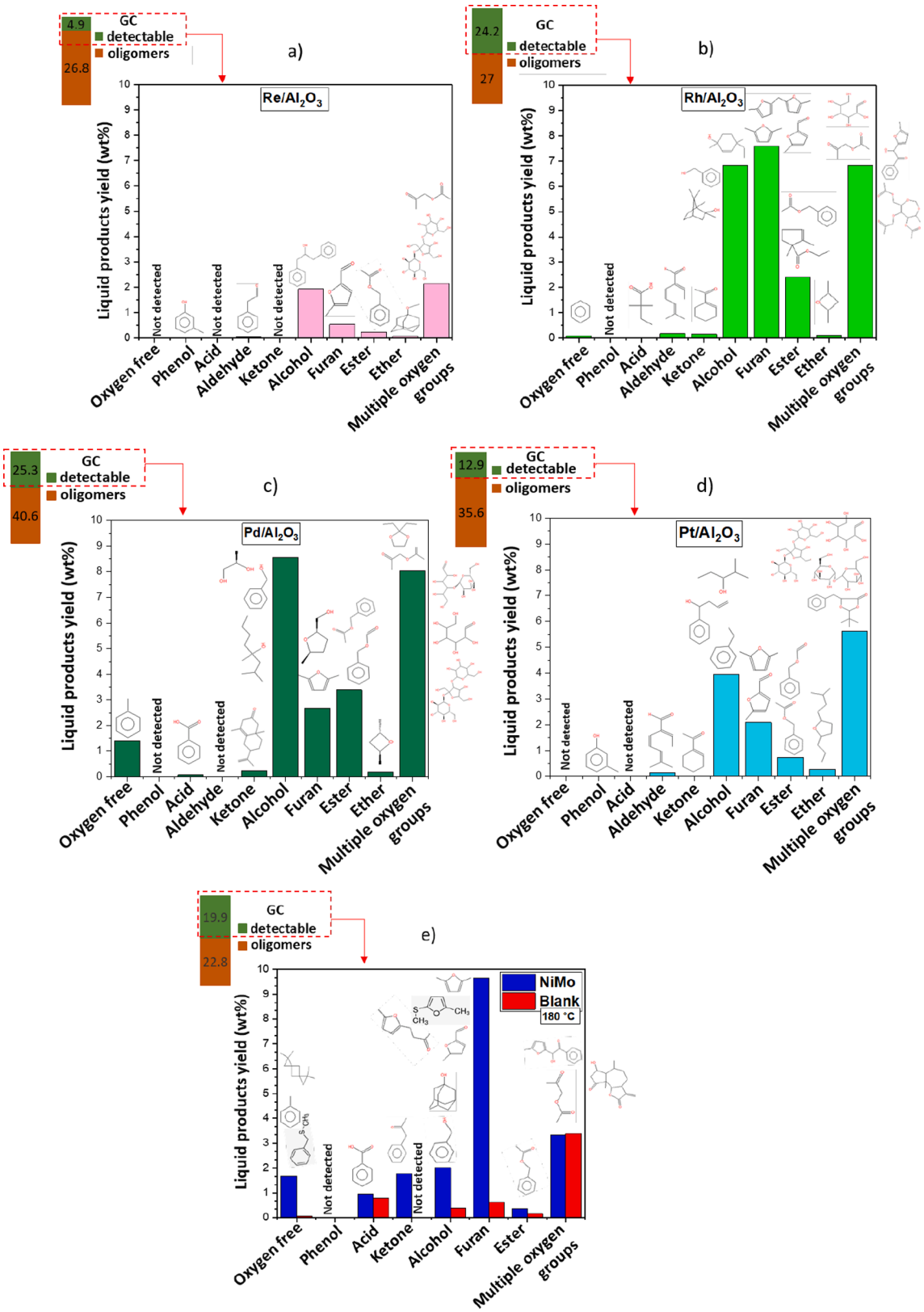

Fig. 3. Distribution of the light liquid product (wt%) produced by thermal and catalytic hydrotreatment of simulated pyrolysis oil using a) Re/Al_2O_3, b) Rh/Al_2O_3, c) Pd/Al_2O_3, d) Pt/Al_2O_3 (a-d 2 wt% metal), e) blank and $NiMo/Al_2O_3$ catalysts at 180 °C and 60 bar H_2.

Al_2O_3 catalysts favour direct HDO [74,75]. The higher yield of water obtained in the presence of $NiMo/Al_2O_3$ also confirms the hydrodeoxygenated products in the GC/MS results. Moreover, in the presence of Rh/Al_2O_3, apart from alcohol, and ester, the yield of multiple oxygen group compounds (made up of sugar derivatives and cross-linked furans and aromatics) was also higher. Rh/Al_2O_3 could also positively suppress the concentration of acid products due to their reaction with alcohols to form esters. It is worth mentioning, based on observations in our

previous work [43], apart from the presence of acetic acid in the feed mixture, acids (e.g. benzoic acid) can also be produced during hydrotreatment reactions via benzaldehyde oxidation to form acid [76,77]. Comparing the acid yields, the NiMo/Al_2O_3 exhibited the highest amount of acid products (about 1 wt%) based on GC/MS results. However, French *et al.* [74] found lower acidity for a sulphided NiMo/Al_2O_3 catalyst than from the noble metal catalysts Pd/C, Pd/char, Pt/char and Ru/char after mild hydrotreatment of pyrolysis oil (150 °C). The reason for this difference could be their lower temperature compared to our experiments.

The use of Pd/Al_2O_3 showed a significant influence on the quantity and composition of the resulting light liquid products (Fig. 3c). The stabilization experiments using Pd/Al_2O_3 showed the highest light liquid yield (25.3 wt%) and also the highest yield of favourable stable alcohols (8.6 wt%), oxygen free hydrocarbons (1.4 wt%) and esters (3.4 wt%). The hydrogenation, cracking and hydrogen transfer reactions that occurred over the Pd/Al_2O_3 consequently resulted in minimizing the solid formation (depicted in Fig. 2). Furthermore, only traces of acids were found and at the same time a quite large amount of esters, suggesting that the Pd/Al_2O_3 was efficient for esterification reactions. Moreover, no phenol and aldehydes were detected, and only minor amounts of ethers and ketones were found. There were no phenols observed as products in any of the experiments, except for Re and Pt but with very low yield, which suggests that the temperature was too low for the hydrogenation and/or hydrogenolysis to produce phenolic compounds. Moreover, the results show that in the presence of Pd/Al_2O_3 at 180 °C low molecular weight oxygen free and stable oxygenated compounds such as toluene, benzyl alcohol and formic acid phenylmethyl ester (FPE) was found as depicted in Fig. 3c. In addition, the largest amount of water was found for Pd/Al_2O_3 and NiMo/Al_2O_3 (Fig. 2), where a higher degree of HDO occurred as evident from the larger amount of oxygen free components (Fig. 3c, and 3e). Water can typically be produced from HDO and condensation reactions: in the former, the oxygenated compounds are converted under H_2 gas to give hydrocarbons, accompanied by water formation. In the latter, two smaller reactive compounds combine to make a larger compound as well as water. The well dispersed Pd/Al_2O_3 and Rh/Al_2O_3 (average metal particle size of 4.4 and 1.9 nm for Pd/Al_2O_3 and Rh/Al_2O_3 catalysts, respectively, see Figure S3), demonstrated promising activity in terms of stabilization of the simulated pyrolysis oil along with reduction in carbon loss as solids. Additionally, a correlation was identified between the light fraction of stabilized oils, as determined by GC–MS data, and the physical appearance of the liquid product samples (stabilized oils), which is further discussed in Supplementary section S6.

To summarize, of all the examined catalysts, Pd/Al_2O_3 is the best candidate due to its ability to: a) achieve the highest conversion, b) greatest yield of liquid product containing both a high amount of hydrocarbons and stabilized oxygenates (exhibiting higher selectivity towards hydrogenation, and HDO), while also demonstrating the lowest carbon loss (char), c) reduced tendency towards undesired reactions (such as condensation, and polymerization), and e) lower propensity of Pd particles to undergo agglomeration compared to other catalysts synthesized under similar conditions.

The composition of the stabilized oils is of great importance to gain a deeper understanding about the performance of various catalysts applied at mild conditions. Accordingly, a comprehensive assessment of the simulated pyrolysis oil feed and stabilized oils was carried out. The H/C, and O/C ratios of these oils as indicators for catalyst suitability via elemental analysis, their average molecular weight (M_w) via GPC analysis as well as their hydroxyl functional groups after a phosphitylation pre-treatment by quantitative P-NMR were determined.

As illustrated in Fig. 4, the elemental composition of stabilized oils from catalytic experiments were compared to simulated pyrolysis oil, and non-catalytic oil, respectively to examine the changes in the composition and the extent of hydrogenation and deoxygenation during mild hydrotreatment with and without catalysts. In the case without catalyst, the liquid product demonstrated reduced O/C and particularly lower H/C ratios (only about 0.9) when compared to the initial feedstock due to dehydration as a typical pathway in non-catalytic pyrolysis oil hydrotreatment [78]. However, catalytic hydrotreatment of the simulated pyrolysis oil provided a lower O/C ratio (<0.3) than for the simulated pyrolysis oil feed (≈ 0.5). Also, values for H/C ratio changed considerably depending on the catalyst applied and they were in the range of 1–1.27, with the highest H/C ratio in the presence of Pd/Al_2O_3 which is similar to that of the feedstock (1.3). This suggests that for catalytic mild hydrotreatment reactions at 180 °C, hydrogen consumption could be attributed to hydrogenation/hydrodeoxygenation of intermediates, likely from dehydration reactions to attain lower oxygen contents. Our results are in agreement with the report in the literature [27] on mild catalytic hydrotreatment of real pyrolysis oil at 250 °C using CoMo/Al_2O_3, Ru/C, and Pd/C with lower H/C ratio of stabilized oil compared to feed. Similarly, compared to a pyrolysis oil feed, Smirnov *et al.* [79] obtained similar H/C ratios for stabilized oil when using a Ni–Cu/SiO_2 catalyst at 190 °C. Furthermore, the results clearly show that the NiMo/Al_2O_3 catalyst performed better than Re/Al_2O_3, Pt/Al_2O_3 and Rh/Al_2O_3 catalysts in deoxygenation of the simulated

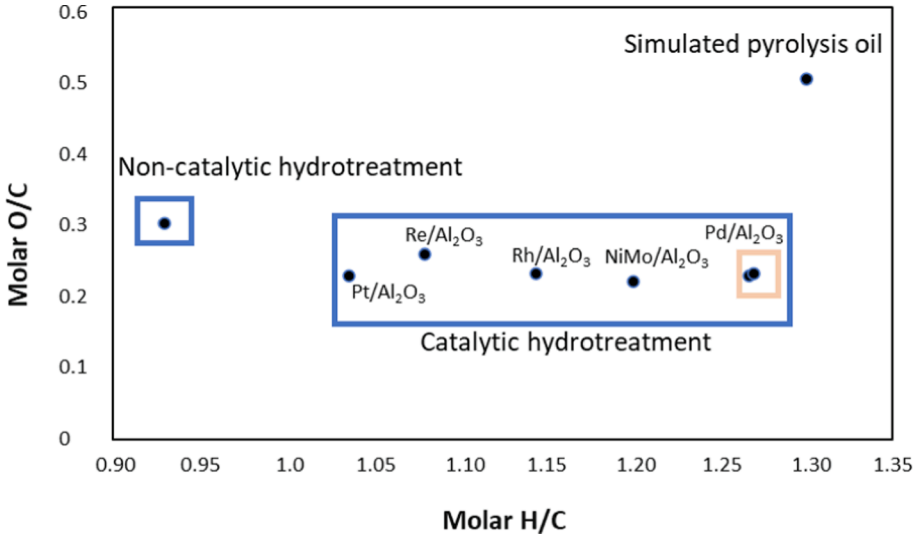

Fig. 4. Van Krevelen plot of the stabilized oils obtained from catalytic mild hydrotreatment of simulated pyrolysis oil over various catalysts. The feedstock (simulated pyrolysis oil) and non-catalytic (blank) oil are given for comparison.

pyrolysis oil under identical reaction conditions tested. In the case of the Pt/Al_2O_3 catalyst though, compared to our results, a lower O/C ratio of stabilized pyrolysis oil derived from Leucaena leucocephala (0.18) were obtained at 300 °C in a study by Payormhorm *et al.* [26]. This difference is likely due to the higher temperature used in their study.

The molecular mass distribution of the simulated pyrolysis oil, liquid and soluble solid products was also assessed using GPC to provide information regarding heavy oligomers obtained from non-catalytic and catalytic hydrotreatment of simulated pyrolysis oil. The molecular weight average (M_w), number average molecular weight (M_n), and molecular weight polydispersity (defined as M_w/M_n) of the liquid products are shown in Table 2. The GPC analysis revealed an increase in the M_w from 360 g/mol for feedstock to over 900 g/mol in the stabilized oils. This observation is in line with GC results indicating the occurrence of oligomerization reactions during the stabilization process. The stabilized oils using Pd/Al_2O_3, Rh/Al_2O_3 and $NiMo/Al_2O_3$ had a higher water content and less oligomers than other stabilized oils as well as non-catalytic oil when determined by GC–MS (Fig. 2). This is in line with the GPC results where lower molecular weights (M_w) were obtained from such oils (Table 2) since the stabilization was more effective. This resulted in less condensation and oligomerization reactions, which increased the concentration of lower molecular weight compounds. Furthermore, an estimate of the average molecular structure of these oils was estimated according to the average molar mass of one monomer unit of feed which is 109 g/mol (details can be found in our previous study [43]). In all experiments except using Pd/Al_2O_3 the produced oils were composed of macromolecules (over 1000 g/mol), among which the stabilized oil from Re/Al_2O_3 contained the heaviest molecules with M_w in the range of 2235 – 2320 g/mol, which corresponds to approximately 20 monomer units. Whereas in the case of Pd, the M_w was significantly lower (933–973 g/mol) which could be represented by nonamers (containing 9 monomer units). This suggests that free radicals formed during mild hydrotreatment underwent different combination reactions [21,78], which produce heavy fractions with particularly greater polydispersities of 1.285 and 1.378 in the absence of a catalyst or in the presence of the Re/Al_2O_3 catalyst, respectively.

Numerous studies have proposed P-NMR to explore the properties of biomass-based green oils [80–83]. In this work, in addition to using GC–MS analysis to characterize and quantify light fractions in the liquid product oils, ^{31}P NMR was employed as well. This complementary technique allowed for a more detailed understanding of the composition of the liquid product, with a particular focus on gaining insights into the structure of the heavy oligomers present in the liquid phase, which could not be detected by GC/MS. Figure S5 shows ^{31}P NMR spectrums of various liquid product oils after being phosphitylated where the chemical shifts for the aliphatic, phenolic, and carboxylic hydroxyls were assigned to 151.6–145, 145–138, and 138–134.6 ranges, respectively, according to the literature [83,84]. The corresponding quantitative data expressed in mmol of OH groups per gr of liquid product oils were also calculated and shown in Fig. 5. According to Figures S5 and 5, a variation of hydroxyl content in uncatalyzed and catalyzed oils can be seen. It is obvious that all oils and particularly catalyzed oil using $NiMo/Al_2O_3$ as well as uncatalyzed oil were rich in phenolic OH groups respectively, whereas only a trace of light phenolic compounds were detected in their composition by GC/MS. These results indicate that phenol groups are more concentrated in the heavy oligomers, and thus there is a tendency for phenolic derivatives to condense or result as products from the formation of heavy oligomers. The lowest content of phenolic OH groups was observed (0.32 mmol/g) when the Pd-1.3 catalyst was used, suggesting its effect on suppression of such condensation reactions. Carboxylic OH units were observed in small amounts for all liquid product oils from noncatalytic and catalytic experiments. In the presence of noble metal catalysts, except Rh-1.8 along with NiMo-3.6,13.2, their amounts were decreased compared to the corresponding uncatalyzed reaction and reached the minimum values using Pt and Pd catalysts, at almost below 0.05 mmol/g. This is in line with GC/MS results, where the yields of light carboxylic groups were very low, while ester yields instead were fairly good due to possible conversion of acids in the presence of alcohols into light esters [40,85]. Even though, in the presence of Rh-1.8, a higher content of carboxylic units comparable to uncatalyzed oil were identified by P-NMR. Interestingly, this was accompanied by the formation of light esters and lack of light acids detected by GC–MS, indicating that Rh catalyzes the formation of carboxylic compounds into heavy oligomers. However, in the presence of NiMo-3.6,13.2, where the greatest quantity of light acids was identified by GC/MS (Fig. 3e), it seems that the relatively high carboxylic OH amount might be primarily associated with the light fraction (Fig. 5). Among oxygen-containing functional group, higher aliphatic hydroxyl units were identified in the uncatalyzed oil as well as catalyzed oil using NiMo-3.6,13.2, while using Pt and Pd catalysts resulted in a slight reduction in the abundance of aliphatic OH groups.

Table 2
Molecular weight distribution and polydispersity of simulated pyrolysis oil and bio-oils produced by its non-catalytic and catalytic (Pd/Al_2O_3, Pt/Al_2O_3, Rh/Al_2O_3, Re/Al_2O_3 and sulphided $NiMo/Al_2O_3$) mild hydrotreatment oil at 180 °C.

Simulated pyrolysis oil and Stabilized oil obtained from		Mw (g/mol)	Mn (g/mol)	Polydispersity (Mw/Mn)
Simulated pyrolysis oil	Feedstock	360	335	1.07
Catalytic oils	Rh-1.8	1866	1783	1.04
	Pd-1.8	953	883	1.09
	Pt-1.8	2252	1973	1.16
	Re-1.9	2277	1783	1.29
	NiMo-3.6,13.2	1987	1725	1.15
	Pd-3.9	1167	996	1.17
Non-catalytic oils	Blank	1804	1317	1.38

3.2.3. Solid products

Solids formation is highly undesirable and limits the yields of the promising bio-oils. Thus, the effect of various metals supported on alumina for suppressing the solids produced was investigated and compared to the blank experiment, as shown in Fig. 6. The highest solid yield was obtained from the blank experiment (27.4 wt%). It is noteworthy to mention that furan ring opening reactions as well as humin formation stemming from furan and sugar derivatives have a large impact on the solid formation [43]. Re/Al_2O_3 showed poor performance in stabilizing the simulated pyrolysis oil, yielding 25.8 wt% solids. Lower solid yield (21.5 wt%) obtained using Pt/Al_2O_3 on the other hand, indicates that the abundance of heavy compounds that could induce polymerization to form solids on the catalyst surface was decreased. This is in line with the higher amount of GC detectable products for Pt/Al_2O_3 as seen in Fig. 2. But still the formed solid content was high, which could be both due to the poorer performance of platinum itself and/or due to Pt particles clustering together on the surface of the catalyst according to its TEM image (Figure S3). Rh/Al_2O_3 was fairly good at stabilizing reactive compounds/intermediates by reducing the formation of solids by half compared to the previous mentioned metals. Interestingly, the solid yield when using the conventional $NiMo/Al_2O_3$ was comparable to Rh/Al_2O_3, and even less than that from using Pt/Al_2O_3 at the same reaction conditions. However, it was reported in the literature that $NiMo/Al_2O_3$ catalysts are less active in hydrotreating real pyrolysis oil and suppressing solids compared to noble metals (Pd, and Pt) due to the absence of sulphur agents in the feed to maintain the catalyst active during the reaction [27]. However, in our experiments a sulphidising agent was added during the experiment, which could be the reason for the observed differences. The result was that some sulphur containing compounds were detected as products with $NiMo/Al_2O_3$ as indicated in Fig. 3e, however the addition of the sulphidising agent in the experiments was not optimized to minimize these byproducts. Pd/Al_2O_3, on the other hand, showed a very low solid yield of only 3.3 wt% and was

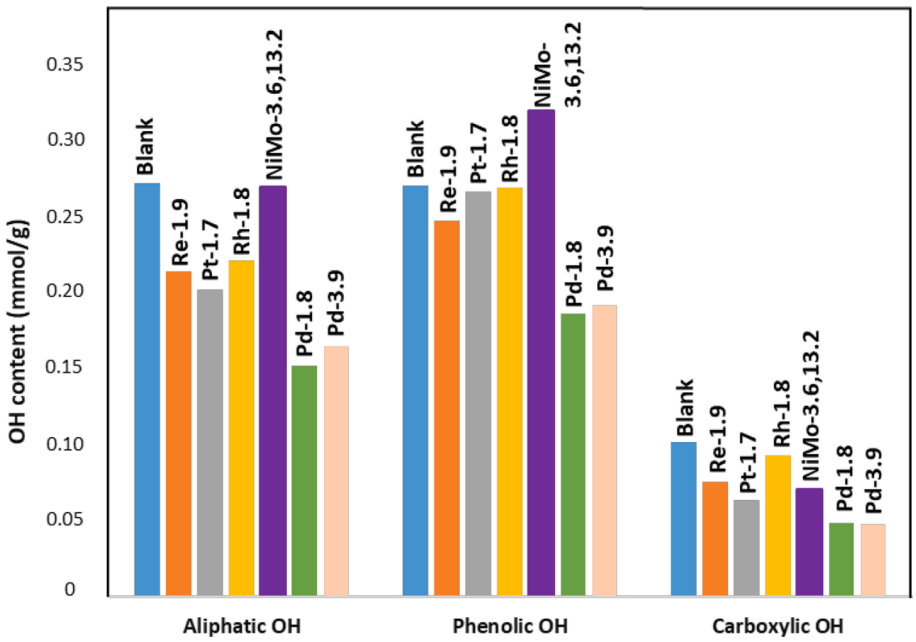

Fig. 5. Hydroxyl group contents of liquid product oils obtained from noncatalytic (blank) and catalytic mild hydrotreatment of simulated pyrolysis oil using various catalysts at 180 °C, and 60 bar pressure determined by quantitative ^{31}P NMR.

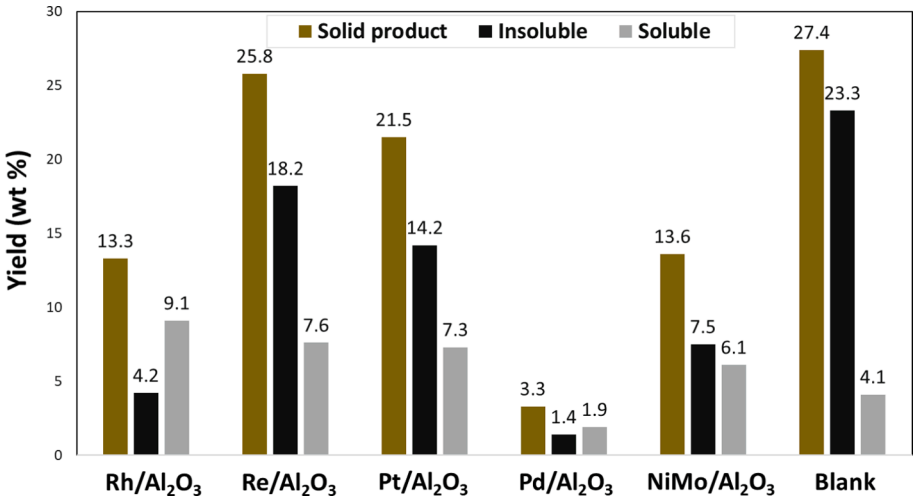

Fig. 6. Solid contents (wt%) obtained from mild hydrotreatment of simulated pyrolysis oil using various catalysts.

thereby the most efficient in reducing carbon loss. This suggests that, in line with previous works [27,86], that Pd/Al_2O_3 has an inhibitory effect on transforming heavy oligomers undetectable by GC/MS into heavy polymers and, thereby into solids.

The evaluation of the solid products was also carried out by separating the produced solids into soluble and insoluble fractions using DMSO solvent, as displayed in Fig. 6. It can be observed that the solid products formed from the thermal experiment and when using Re/Al_2O_3, Pt/Al_2O_3 and $NiMo/Al_2O_3$ consisted of high insoluble fractions. However, the amount of the insoluble fraction in the solid phases are lower for Pd/Al_2O_3 and Rh/Al_2O_3. This indicates that both catalysts provide an inhibitory effect for the further conversion of soluble solids/polymers into heavier insoluble solids/polymers. Overall, the distribution trend observed for the product and the composition of the liquid product indicate that stabilization of the simulated pyrolysis oil using different metals supported on alumina proceeds through a sequence of steps as depicted in Scheme 1, which will be discussed in Section 3.4.

3.2.3.1. Soluble solids composition. Soluble solids refer to the ability of solid substances to dissolve into solvents like DMSO. To determine the composition and average M_w of the DMSO soluble solids, 2D-HSQC-NMR and GPC were performed and the results are illustrated in Fig. 7 and Table 3. It is obvious that various chemical compositions for the soluble solids were obtained using different catalysts comprising aliphatic, aromatic, ferulate esters and sugar compounds (Fig. 7). The aliphatic C–H bonds, sugars, aromatic C–H bonds, and ferulate esters display peaks approximately in the ranges of δC/δH 5–55/0.5–3.8, 48–105/3–5.5, 110–125/6.2–7.5, and 122–135/6.7–7.8 ppm, respectively according to literature [87]. In the presence of Rh/Al_2O_3 and Pd/Al_2O_3 catalysts, 2D-HSQC-NMR spectrums present sugar and aliphatic functional groups with comparable peaks. Also, in the presence of $NiMo/Al_2O_3$ catalyst, soluble solids with similar functional groups were formed, and complex saccharides along with aliphatics were abundantly produced. In the absence of catalyst as well as in the presence of Re/Al_2O_3 and Pt/Al_2O_3 catalysts, apart from aliphatic and sugar components, heavier aromatics and ferulate esters were also present in soluble

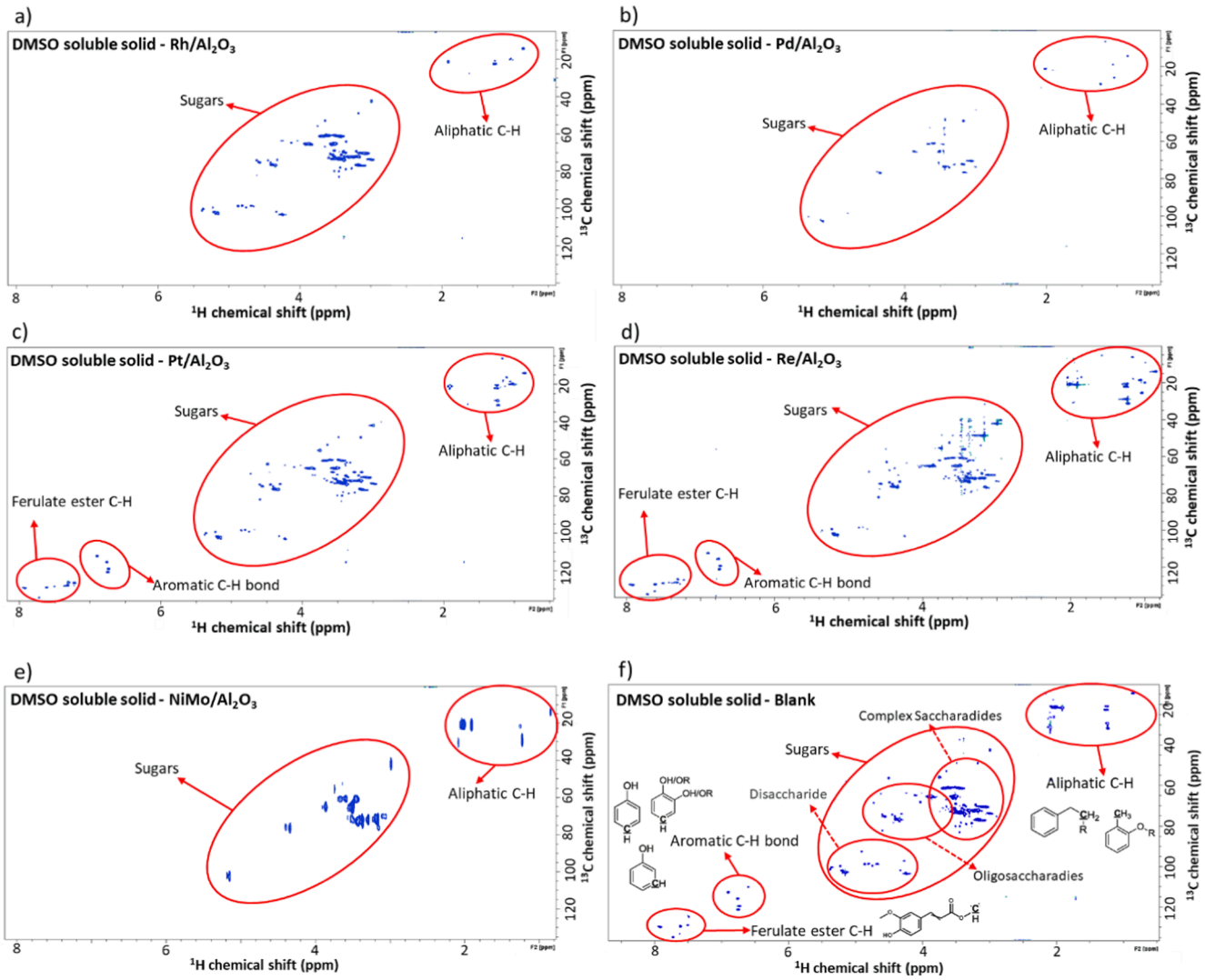

Fig. 7. The composition of soluble solids obtained from mild hydrotreatment of simulated pyrolysis oil using various catalysts: a) Rh/Al_2O_3, b) Pd/Al_2O_3, c) Pt/Al_2O_3, d) Re/Al_2O_3, e) $NiMo/Al_2O_3$ and f) blank.

Table 3
Molecular weight distribution and polydispersity of soluble solids formed by non-catalytic and catalytic mild hydrotreatment of simulated pyrolysis oil over Pd/Al_2O_3, Pt/Al_2O_3, Rh/Al_2O_3, Re/Al_2O_3 and sulphided $NiMo/Al_2O_3$ catalysts at 180 °C.

Soluble solid obtained from		M_w (g/mol)	M_n (g/mol)	Polydispersity (M_w/M_n)
Catalytic runs	**Rh-1.8**	2761	1856	1.46
	Pd-1.8	3054	2126	1.43
	Pt-1.8	3531	2469	1.44
	Re-1.9	4280	2754	1.55
	NiMo-3.6,13.2	3195	2256	1.46
	Pd-3.9	2360	1858	1.26
Non-catalytic run	**Blank**	4044	849	4.78

solid composition. This observation indicates the occurrence of distinct reaction pathways compared to those identified using the catalysts mentioned earlier which yielded components with heavier structures. Notably, the intensity of these peaks with Re/Al_2O_3 and without catalyst were more pronounced. According to 2D-HSQC-NMR results, the soluble solid formation can be achieved through several ways, either sugars and aliphatic compounds together, or a combination reaction occurring between sugars, aliphatics, esters and aromatics.

As can be seen in Table 3, the average M_w determined by GPC is strongly correlated with the type of catalysts employed. In line with observations derived from the 2D-NMR spectrums for soluble solids, the highest average molecular weights (M_w) were obtained for the soluble solids using Re-1.9, and Pt-1.8 catalysts and without catalyst, with the ranges of 4288–4273, 3578–3485, and 4059–4030 g/mol, respectively. This increase is likely attributed to the presence of heavy aromatics within their structure. It was also accompanied by the highest polydispersity, particularly for the soluble solids derived without catalyst (4.78). It suggests that higher selectivity towards heavier molecules formation occurs in the absence as well as presence of Re-1.9, and Pt-1.8 catalysts. In the presence of other catalysts, including, NiMo-3.6,13.2, Pd-1.8 and particularly Rh-1.8, lower M_w soluble solids were obtained (<3200 g/mol), where ferulate ester and aromatic functional groups were absent (Fig. 7a, 7b, and 7e). Out of these, the M_w of the soluble solid derived with NiMo-3.6,13.2 was higher (3177 – 3213), potentially attributed to the presence of a greater number of peaks in sugar and aliphatic regions. Interestingly, despite the variability in the yield of soluble solids derived from these catalytic reactions (Fig. 6), the findings illustrate the comparable and impressive catalytic effectiveness of these catalysts in restraining the formation of heavy soluble polymers (and indeed lowering M_w) which can be further polymerized to heavier

insoluble polymers/solids. This observation is consistent with their lower polydispersity values, ranging from 1.43 to 1.46 (Table 3), and their elevated yields of lighter fractions in their liquid phases, evidenced by GC/MS results (Fig. 2).

3.2.3.2. Insoluble solids composition. The solids insoluble in DMSO are composed of highly extensive structures, making them resistant to dissolution. Consequently, the insoluble portion of the total solid is limited to compositional analysis, with techniques like CHOS elemental analysis being employed for this purpose. The elemental compositions of the insoluble solids in DMSO (char) obtained from uncatalyzed and catalyzed mild hydrotreatment of simulated pyrolysis oil at 180 °C, 60 bar after 4 h reaction were determined and are presented as carbon/hydrogen ratios (C/H) in Table 4. The results show that the characteristics and composition of char are influenced by the presence and types of catalyst. As expected, the carbon content in the insoluble solid was increased in the absence of catalyst and a C/H ratio of 1 was acquired where lower yields of liquid (with lowest H/C molar ratio), and soluble solid (Fig. 2f, and Figs. 4, and 6) were identified. This is attributed to a greater degree of polymerization reactions occurring without the catalyst, originating from reactive oxygenates such as furanic and sugar compounds [43,46] which resulted in formation of fully developed char. In the presence of catalysts, on the other hand, insoluble solids with different properties were recognized where the C/H molar ratios were reduced to less than 0.75 (Table 3). This indicates the efficiency of catalysts, particularly Pd and Rh in suppressing the formation of highly polymerized species and stabilizing reactive intermediates to catalyse hydrocracking, hydrogenation and HDO reactions with higher yields of stabilized oils (Fig. 3). This is also coupled with higher yields of soluble solids with lighter polymers as illustrated in Fig. 6. These reactions, especially with well dispersed Pd as well as Rh (see Figure S3), occurred thanks to their capacity to selectively cleave and hydrogenate C-O bonds in a variety of monomeric, dimeric, oligomeric and light polymeric molecules. Interestingly, NiMo-3.6,13.2 showed better performance compared to Re and Pt in reducing the carbon content according to the CHOS elemental analysis and yielding C/H ratio of 0.7 compared to 0.73–0.75 for Re and Pt. Compared to the uncatalyzed insoluble solid, the inhibitory effect of catalysts on carbon loss as insoluble solids during stabilization of simulated pyrolysis oil at mild condition, caused the char to be less fully developed.

Thus, so far, the effect of different noble metals, Re and NiMo catalysts have been investigated for stabilization of simulated pyrolysis oil and compared with that of the corresponding blank experiment. Of the catalysts examined, Pd/Al_2O_3 was then selected for further analysis because it showed the most promising results in terms of the highest degree of stabilization.

In addition, the effect of Pd loading was studied by comparing two Pd/Al_2O_3 samples with 1.8 and 3.9 wt% Pd. The results can be found in the Supplementary material Section S7. Increasing the palladium loading gave a slightly higher bio-liquid yield, but the solid formation increased. The loss of carbon in the solids, in combination with the high price of palladium, indicates that lower palladium loading is more beneficial.

Table 4
Elemental Composition of insoluble solids formed during mild hydrotreatment of simulated pyrolysis oil in the absence and presence of various catalysts at 180 °C, 60 bar and 4 h.

Insoluble solids	Blank	NiMo-3.6,13.2	Re-1.9	Pt-1.7	Rh-1.8	Pd-1.8	Pd-3.9
C/H molar ratio	1.00	0.70	0.75	0.73	0.58	0.56	0.46

3.3. Stability of simulated pyrolysis oil

To measure the stability of the simulated pyrolysis oil during aging, the accelerated aging method used by NREL group [24], was employed to artificially expedite the natural aging process. The same simulated pyrolysis oil mixture used in the reaction condition, containing 6 model compounds in 150 ml hexadecane as a solvent, was exposed to 80 °C for 2 h under nitrogen gas in a 450 ml Parr reactor. In our prior work, we found a large contribution of HMF, and levoglucosan to polymerization reactions during the heat treatment of simulated pyrolysis oils up to 180 °C [43]. We therefore also prepared a mixture of 4 model compounds-excluding sugar and furanic compounds- in an appropriate amount of solvent. This mixture underwent aging at identical experimental conditions as used for the six-model compound simulated pyrolysis oil and obtained aged oils denoted as '*Aged-feed 6*' and '*Aged-feed 4*', respectively. During aging, simulated pyrolysis oil spontaneously separated into two phases containing a dense brownish fraction and a yellowish phase with hexadecane-soluble compounds, while no solids were obtained. This suggests the presence of multiple reactions like condensation, esterification, polymerization, etc., possibly due to interactions among the reactive compounds [88]. It was also found that the quantity of the dense phase depends on the type of the feedstock, where a lower amount of dense phase was seen from the feedstock from which HMF and levoglucosan were removed. To understand the changes occurring in the aging process, the composition of fresh and aged oils from these two experiments were compared using GC/MS, P-NMR and Karl Fischer and the results are presented in Figs. 8 and 9 and Figure S9 and Table 5, respectively.

No water was detected for these two aged oils (Fig. 8a and 8b) aligning with Boucher *et al.*'s observation of no significant changes in water content during accelerated aging of softwood bark-derived pyrolysis oil [89]. According to the GC results (Table 5), all model compounds underwent conversion during the accelerated aging process through reactions such as self-condensation, esterification, aldol condensation, and phenol, and aldehyde reactions [25,90]. The conversions observed for guaiacol, and benzaldehyde were lower (52 and 60 %, for *Aged-feed 6*), while complete conversion of both HMF and levoglucosan were observed. In the case of *Aged-feed 4*, although no reactive compounds like HMF and levoglucosan were present, similar conversions were observed for acetic acid and guaiacol compared to *Aged-feed 6*. However, the conversion of hydroxyacetone and especially benzaldehyde was notably higher in *Aged-feed 6* compared to *Aged-feed 4*. This difference is likely due to the potential of HMF to undergo aldol condensation with benzaldehyde under acid-catalyzed conditions [91], along with condensation and oligomerization reactions involving sugars and aldehydes [43]. Additionally, crosslinking between the generated reactive intermediates and aldehyde and/or hydroxyacetone could also contribute to this phenomenon. Importantly, during the accelerated aging process, all model compounds presented in both feed samples, only converted to heavy oligomers as no light compounds were detected by GC (Fig. 8a and 8b).

To understand chemical changes occurring in simulated pyrolysis oil after accelerated aging, ^{31}P NMR analysis was utilized to quantify the

Table 5
Conversion of various model compounds along the aging period of simulated pyrolysis oils and during mild hydrotreatment (stabilization) of aged-simulated pyrolysis oil in the presence of Pd/Al_2O_3 catalyst at 180 °C, 60 bar and 4 h. *Total conversion based on inlet feed with 6 components before aging.

Conversion (wt%)	Aged feed 4	Aged feed 6	Stabilized-aged feed 6*
Acetic acid	76	75	96
Hydroxyacetone	79	95	99
Guaiacol	47	52	61
Benzaldehyde	32	60	83
HMF	–	100	100
Levoglucosan	–	100	100

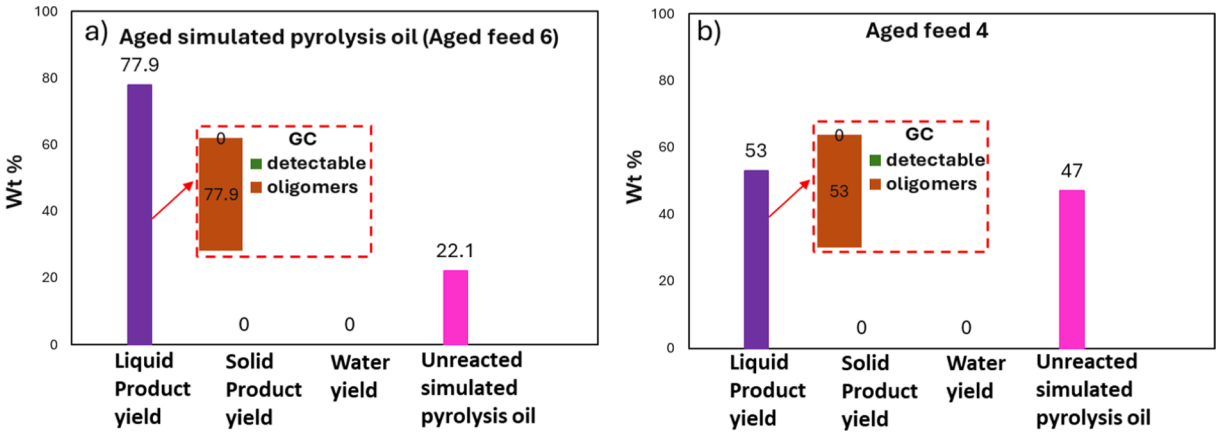

Fig. 8. Comparison of products yield (wt%) from aging process: a) aging of simulated pyrolysis oil containing 6 compounds, b) aging of simulated pyrolysis oil containing 4 compounds.

content of the hydroxyl compounds and the results are shown in Figure S9 and Fig. 9. Comparing P-NMR spectra of fresh and aged simulated pyrolysis oils revealed differences in peaks, indicating alterations in the composition and structure of the oil. As can be seen in Fig. 9, all three types of hydroxyl-containing functional groups decreased after aging, aligning with the conversion or transformation of OH-containing model compounds present in simulated pyrolysis oil. This decline in OH content is associated with the degradation and transformation of oxygen-containing functional groups during the aging process, into heavier compounds like oligomers that may not contain any OH groups. This decreasing trend after aging is consistent with findings from stability tests conducted on pyrolysis oil by Ben *et al.* [92]. Interestingly, the OH groups from aliphatic and phenolic compounds were only reduced by 9 and 19 %, respectively. However, the conversion of the model compounds in the simulated pyrolysis oil was significantly larger suggesting that a large amount of hydroxyls remained in the heavy oligomers.

Moreover, to examine the behaviour of *Aged-feed 6* during catalytic stabilization with Pd/Al_2O_3, it was compared to that of fresh simulated pyrolysis oil under same reaction conditions (180 °C, 4 h, 60 bar H_2 pressure), see Fig. 10. In addition, the results are compared with an experiment where stabilization was followed by the aging procedure and the results are shown in Fig. 10c. For the case with stabilization followed by aging (Fig. 10c), the solids were removed after stabilization together with the catalyst. No more solids were formed during aging on the stabilized oil. Thus, the solids from the stabilization of fresh oil (Fig. 10a) and stabilization followed by aging (Fig. 10c) should be the same. However, stabilization followed by aging exhibited higher solid formation, i.e. 5.1 % compared to 3.3 %. The reason for this difference could be that there were small modifications made on the reactor for the experiments with aging prior to and after stabilization (Fig. 10b and 10c). In addition, a new catalyst batch were used for the experiment with stabilization followed by aging (1.9 % Pd/Al_2O_3, Fig. 10c) compared to 1.8 % Pd/Al_2O_3 for the other two experiments (Fig. 10a and 10b). However, it is very clear that when conducting the aging of the simulated pyrolysis oil followed by the stabilization experiment (Fig. 10b) it resulted in a further increase in solid yield to 9.1 %. Moreover, the conversion of the feed increased for both aging prior to and after stabilization, which likely is due to oligomerization reactions during aging.

To conclude, stabilization can be an important measure for storage of pyrolysis oil to reduce the solid formation. We suggest the reason for this is that during aging, large oligomers were formed as evident by the GC/MS analysis (Fig. 8) and that during the HDO some of these oligomers are transformed into solid residues.

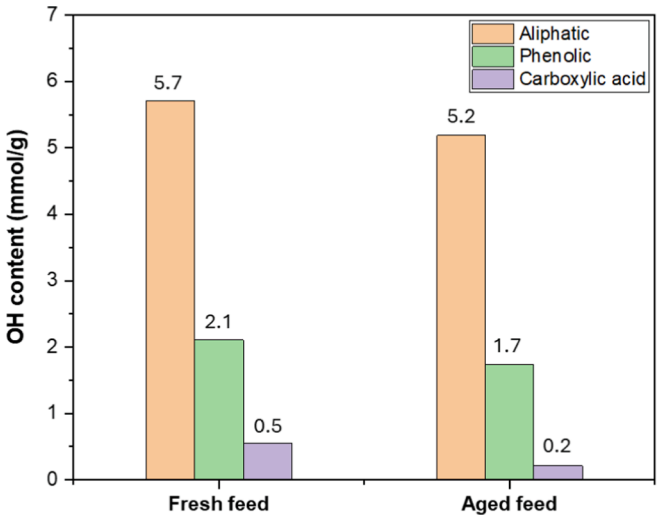

Fig. 9. Hydroxyl group contents of fresh and aged-simulated pyrolysis oil during accelerated aging process determined by quantitative ^{31}P NMR.

3.4. Reaction pathway

Based on our work on various metal alumina supported catalysts, several reaction pathways can be distinguished. However, the intermediates produced during the reaction, varied depending on the metal type and loadings. Scheme 1 presents a proposed reaction network for the catalytic mild hydrotreatment of simulated pyrolysis oil at 180 °C, defining abbreviations that will be used in the discussion below for detected compounds. These are general classes of reactions, but of course there can exist many more in such a complex reaction mixture. Light compounds in the liquid product detected by GC/MS are shown in the green box. They contain monomers with different functional groups, as well as compounds produced from condensation reactions such as multi-oxygenated compounds. These reactive compounds undergo oligomerization which leads to the formation of higher molecular weight soluble oligomers in the liquid phase and thereafter upon further condensation yield polymers/solids. This route mainly occurs in the non-catalytic process, where the polymer and solid formation was enhanced, likely due to the formation of a large amount of reactive compounds. According to the GC/MS results, similar compounds were found in the presence of various catalysts but with different concentrations, although some of them were produced only by some specific catalysts, which will be discussed in detail in the following paragraphs.

In our previous study [43] we found that HMF and levoglucosan

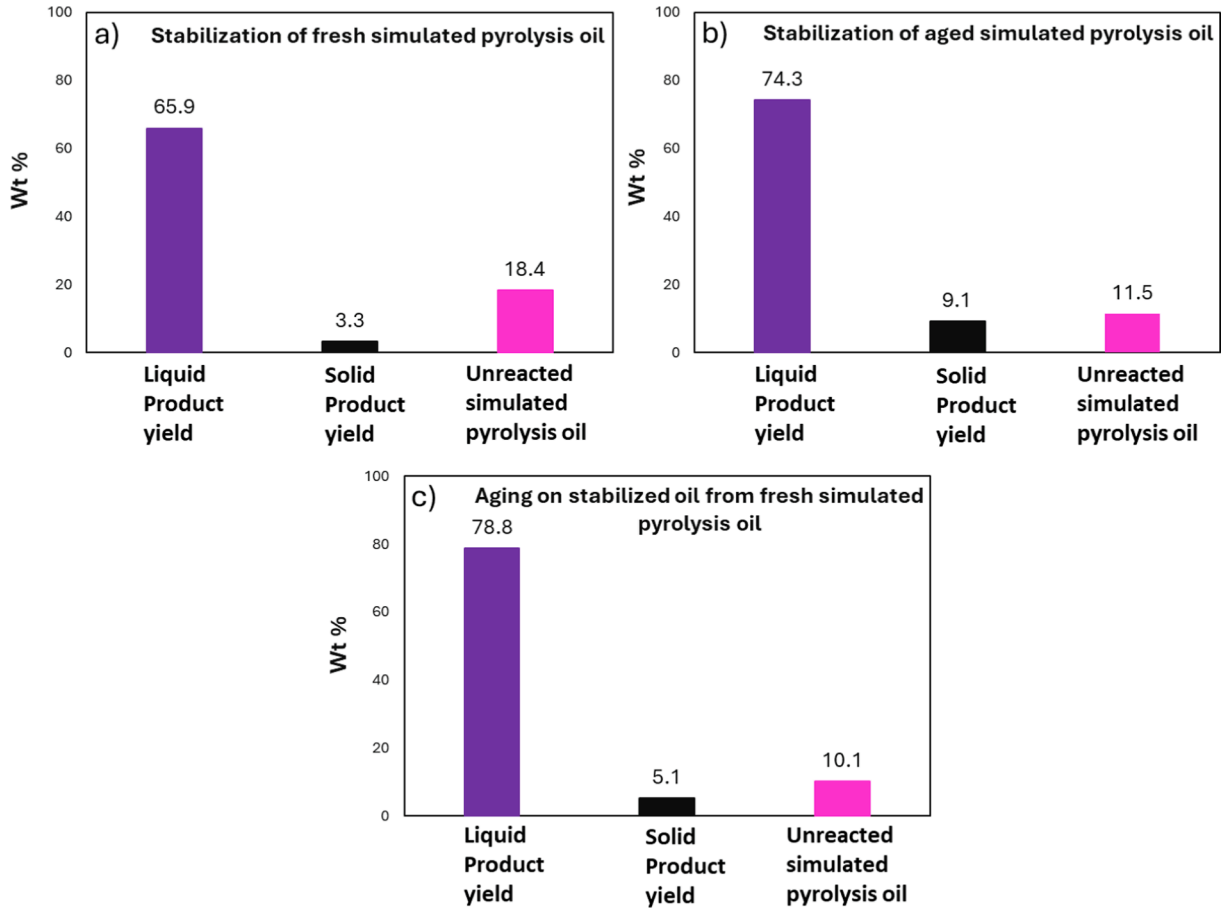

Fig. 10. Comparison of yields (wt%) for liquid and solid products and the amount of unreacted simulated pyrolysis oil. Stabilization reactions were performed at 180 °C under 60 bar H_2 for 4 h and 1 g Pd/Al_2O_3 catalyst. Three cases are compared, stabilization only, aging + stabilization and stabilization + aging.

were the most reactive compounds in the feedstock mixture. The reaction products from HMF were many furanic intermediates and even products of crosslinking with other oxygenated compounds such as sugar and benzaldehyde/guaiacol derivatives. This concurs with the literature, which reported the potential for cross-polymerization reactions between furan, sugars and phenols [45,46]. As can be seen in Scheme 1, formation of HMP and Melezitose confirms the occurrence of these kinds of reactions resulting from HMF derivatives cross-linking with benzaldehyde/guaiacol and sugar derivatives, respectively. Moreover, MF, MFA and DMF are other furanic compounds produced from HMF according to the possible reaction pathways during the mild hydrotreatment as displayed in Scheme 1. MF, MFA, DMF, and MF with high reactivity was predominant when using Re/Al_2O_3, and Pt/Al_2O_3. However, in the presence of the Pd/Al_2O_3 catalyst, and particularly at higher loadings (3.9 wt%), the formation of stable DMF was the dominant path, along with hydrogenation of the furan ring, formed FAT. It should be noted that FAT was not observed in the presence of the other catalysts employed in this study. In addition, HMF was also transformed into the compounds FME, and BMF via condensation, giving higher concentrations in the presence of the Re/Al_2O_3 catalyst compared to other catalysts. In the case of $NiMo/Al_2O_3$ and Rh/Al_2O_3 a variety of furanic compounds containing both reactive and stable furans were observed, in which DMF was the main compound. Another possible pathway for HMF conversion is the ring-opening reaction that occurs during hydrotreatment, leading to the formation of LA as an intermediate, followed by hydrogenation and reactions with alcohol and ketone to produce ethers DD and ODT, respectively which is previously reported [93]. However, only trace amounts of ethers were formed in all catalytic experiments using various catalysts, suggesting that this reaction path is not dominating under the conditions used.

Many different oxygenates and oxygen free compounds were produced from benzaldehyde via hydrogenation, HDO, condensation and dehydrogenation. GC/MS detected both benzoic acid and benzyl alcohol, which most likely arise from benzaldehyde oxidation and hydrogenation, respectively. It should nevertheless be noted that the acid was formed mainly when $NiMo/Al_2O_3$ catalyst was used. However, all catalysts were selective towards benzaldehyde hydrogenation to benzyl alcohol. It should be noted that a high yield of alcohols, composed mostly of benzyl alcohol, was obtained when using Pd/Al_2O_3 and Rh/Al_2O_3, suggesting that a notable amount of benzaldehyde was converted into alcohols in these cases. These reactions can be followed by converting benzyl alcohol into toluene via hydrodeoxygenation, although this oxygen-free compound can also be produced from guaiacol hydrotreatment, as shown in previous studies [33,94]. The lack of oxygen-free compounds using Re/Al_2O_3 and Pt/Al_2O_3, shows that the HDO step did not occur in the presence of these catalysts although, toluene was seen using other noble metals as well as $NiMo/Al_2O_3$ catalysts but with higher yield for $NiMo/Al_2O_3$. The ester APE was produced from benzaldehyde derivatives through condensation reaction with acetic acid. APE was produced in all catalytic experiments, and with a higher yield when using Pd/Al_2O_3, and Rh/Al_2O_3.

Apart from the contribution of acetic acid or its intermediates in the mixture with alcohols to generate esters, it is also possible that acetic acid (or its intermediates in the mixture) react with phenol produced from guaiacol hydrogenation to produce the relevant ester FPE. Moreover, acetic acid could be hydrogenated into acetone [95] and contribute to condensation reactions such as self-aldol condensation [76]. These reactive condensates are prone to promote further reactions

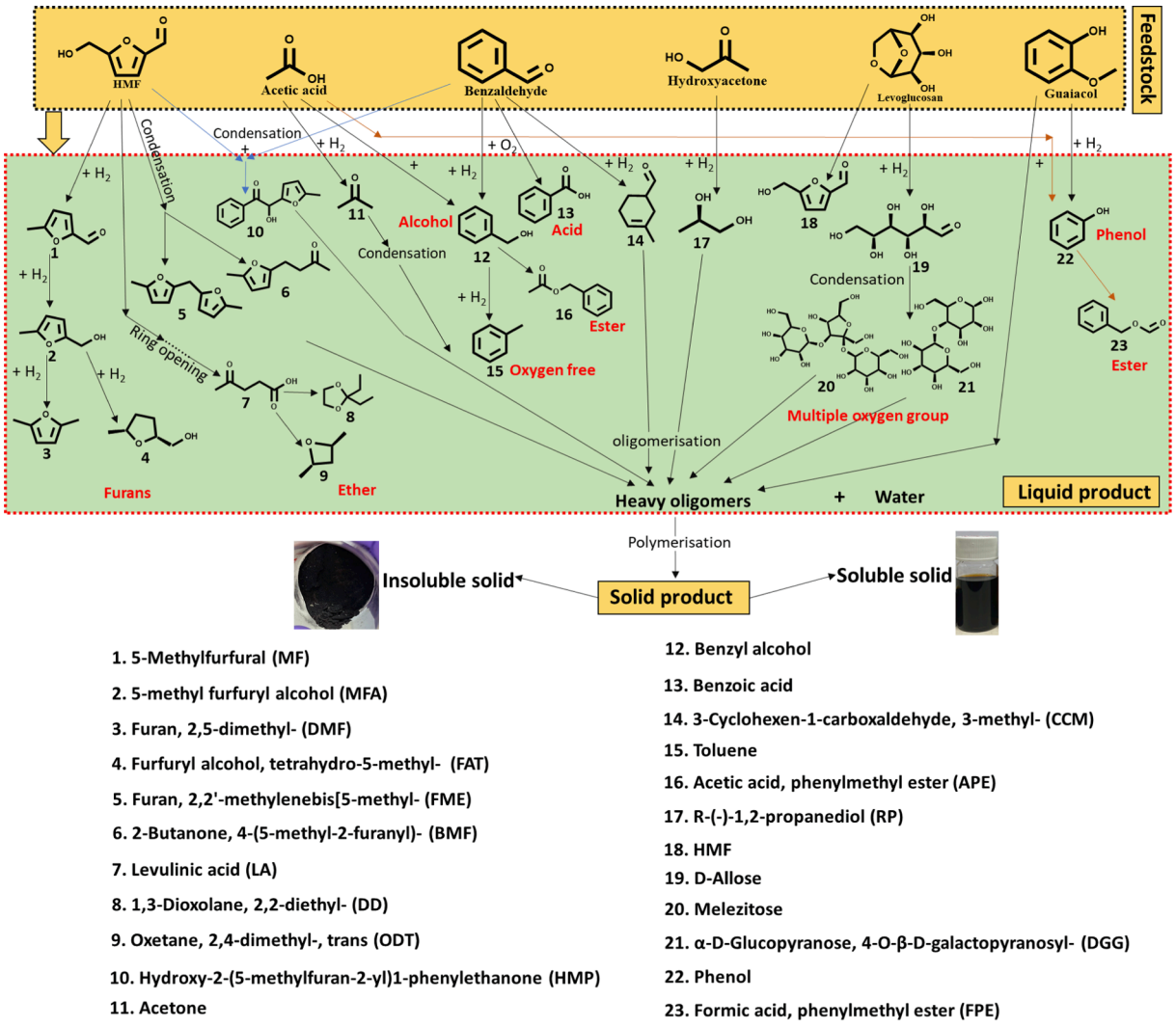

Scheme 1. Reaction pathways proposed for the catalytic mild hydrotreatment of simulated pyrolysis oil at 180 °C. Reactions are suggested in accordance with the products identified by GC/MS, including trace compounds and their formation due to the likely reaction classes discussed in the text.

to generate heavy soluble oligomers [76].

The ketone hydroxyacetone, is probably hydrogenated into RP [38] but may also interact with other reactive intermediates and initiate oligomerization reactions. Hydroxyacetone not only contributes to hydrogenation reactions to generate relevant alcohols but also plays an important role in condensation and thus oligomerization reactions. Due to the complexity of the liquid product mixture, explaining all further reaction possibilities regarding hydroxyacetone is challenging.

Levoglucosan is another compound with high reactivity and could be dehydrated into HMF [12,56] and undergo a ring-opening reaction [68] to produce reactive D-allose, as well as undergo condensation to form melezitose and DGG that then induces oligomerization reactions. Ethers such as DD can also be produced from sugar due to its conversion to HMF. Comparing different catalysts, the higher yields of compounds with multiple oxygen groups in the liquid product (Fig. 3) resulting from condensation of sugar derivatives were obtained in the presence of Rh/Al_2O_3, Pd/Al_2O_3 and Pt/Al_2O_3. Some of the multiple oxygen group compounds were thereafter further converted into heavy oligomers (undetectable by GC) and then polymers/solids. Furthermore, another possible reaction pathway for sugar derivatives using noble metals is their hydrogenation at mild conditions to generate alcohols [96,97].

Guaiacol as a representative of phenols, showed low activity at this rather low temperature. According to GC/MS results, a trace of phenolic compounds was detected when Ru/Al_2O_3, Re/Al_2O_3, Pd/Al_2O_3, and Pt/Al_2O_3 were applied, whereas phenolic OH units were abundant in heavy oligomer products according to P-NMR. It seems possible then that guaiacol was predominantly involved in condensation and oligomerization reactions that contributed to heavy compounds not detectable by GC/MS.

4. Conclusions

Mild hydrotreatment of simulated pyrolysis oil has been examined at depth in this work for the stabilization (hydrogenation and cracking) and polymerization reactions of simulated pyrolysis oil in a batch reactor using Pt/Al_2O_3, Pd/Al_2O_3, Rh/Al_2O_3, Re/Al_2O_3 and NiMo/Al_2O_3. It was found that Pd/Al_2O_3 was the most efficient catalyst of the materials studied. It exhibited the highest yield of a bio-liquid comprised of oxygen-free and stabilized oxygenated compounds, such as toluene, hydrogenated furan (DMF and FAT), esters (APE and FPE) and alcohols (benzyl alcohol and RP), along with the lowest level of polymerization and thus solid products (3.3 wt%). Rh/Al_2O_3 was also active in catalyzing the selective conversion of reactive compounds into more stable light oxygenates, with quite high yield of the bio-liquid, but with a significantly higher yield of solids (13.3 wt%). Notably distinct solid compositions were identified with Pd and Rh, primarily consisting of soluble polymers/solids enriched in aliphatic and sugar derivates. However, following the Pt/Al_2O_3 catalyst, Re/Al_2O_3 rendered the lowest

yields and qualities of the liquid product, comprised mainly of heavy oligomers rich in phenolic compounds, without deoxygenated light compounds, which led to both polymerization and carbon loss with mainly heavy insoluble polymers being enhanced remarkably. Some of the noble metals (Pt, Rh and Pd) and Re were efficient in reducing acids in the light oil: Pt/Al_2O_3 and Rh/Al_2O_3 in particular had the highest conversion of acetic acid and virtually no acids were found in the light product. The sulphided $NiMo/Al_2O_3$ catalyst, on the other hand, achieved a yield of liquid product of 42.7 wt%, comprised up of 47 % light compounds but with more acids as products and with quite high solid formation. The most efficient catalyst, i.e. Pd/Al_2O_3 exhibited the least amount of solids and the amount of these solids that were insoluble were only 1.4 wt%. The Pd loading was further increased from 1.8 wt% to 3.9 wt%, which resulted in slightly higher liquid yield, however the solid formation increased. Thus, considering the loss of carbon in the solids, as well as the high price of palladium, a lower loading is more beneficial.

The stability of simulated pyrolysis oil was assessed via an accelerated aging process performed at 80 °C for 2 h. It can be concluded from the experiments that significant reactions occurred during the aging, primarily involving oligomerization. HMF and levoglucosan were completely converted during the aging, but also the other components (acetic acid, hydroxyacetone, guaiacol and benzaldehyde) were converted to a large extent. The lowest conversion was found for guaiacol, with 52 % conversion. Moreover, the aging was also performed in the absence of sugar and furanic compounds, which were the most reactive components. For this case the overall reactivity was lower, however the conversion was still significant. Hydroxyacetone was the most active compound when using four components, with a conversion reaching 79 %. Interestingly, benzaldehyde exhibited significantly higher activity in the presence of HMF and/or levoglucosan, suggesting reactions occur between those compounds. For both aging processes, large oligomers were formed that could not be detected by GC/MS. The aged-simulated pyrolysis oil was stabilized using the Pd/Al_2O_3 catalyst and compared with the stabilization first followed by aging. The solid amount increased from 5.1 to 9.1 % when aging the pyrolysis oil followed by stabilization compared to the opposite order. We suggest that the reason for this result is the formation of oligomers during aging which could be further transformed to solids. These results show the importance of stabilizing the pyrolysis oil, since upgrading of aged pyrolysis oil causes larger problems due to the formation of more solids.

CRediT authorship contribution statement

Elham Nejadmoghadam: Writing – original draft, Methodology, Investigation, Formal analysis, Data curation, Conceptualization. **Abdenour Achour:** Supervision, Conceptualization. **Olov Öhrman:** Writing – review & editing, Supervision, Funding acquisition, Conceptualization. **Muhammad Abdus Salam:** Supervision. **Derek Creaser:** Writing – review & editing, Supervision, Conceptualization. **Louise Olsson:** Writing – review & editing, Supervision, Methodology, Funding acquisition, Conceptualization.

Declaration of competing interest

The authors declare the following financial interests/personal relationships which may be considered as potential competing interests: Olov Öhrman reports financial support was provided by Preem AB. If there are other authors, they declare that they have no known competing financial interests or personal relationships that could have appeared to influence the work reported in this paper.

Data availability

Data will be made available on request.

Acknowledgements

This work has been performed at the Competence Centre for Catalysis (KCK) and the Chemical Engineering division at the Chalmers University of Technology in collaboration with Preem. The Competence Centre for Catalysis is hosted by Chalmers University of Technology and financially supported by the Swedish Energy Agency (Project No. 52689-1) and the member companies Johnson Matthey, Perstorp, Powercell, Preem, Scania CV, Umicore, and Volvo Group.

Appendix A. Supplementary material

Supplementary data to this article can be found online at https://doi.org/10.1016/j.enconman.2024.118570.

References

[1] Figueirêdo MB, Hita I, Deuss PJ, Venderbosch RH, Heeres HJ. Pyrolytic lignin: A promising biorefinery feedstock for the production of fuels and valuable chemicals. Green Chem 2022;24:4680–702. https://doi.org/10.1039/D2GC00302C.
[2] Zhang M, Wu Y, Han X, Zeng Y, Xu CC. Upgrading pyrolysis oil by catalytic hydrodeoxygenation reaction in supercritical ethanol with different hydrogen sources. Chem Eng J 2022;446:136952. https://doi.org/10.1016/j.cej.2022.136952.
[3] Yaman S. Pyrolysis of biomass to produce fuels and chemical feedstocks. Energy Convers Manag 2004;45:651–71.
[4] Zhang Q, Chang J, Wang T, Xu Y. Review of biomass pyrolysis oil properties and upgrading research. Energy Convers Manag 2007;48:87–92.
[5] Qiu B, Tao X, Wang J, Liu Y, Li S, Chu H. Research progress in the preparation of high-quality liquid fuels and chemicals by catalytic pyrolysis of biomass: A review. Energy Convers Manag 2022;261:115647.
[6] Lahijani P, Mohammadi M, Mohamed AR, Ismail F, Lee KT, Amini G. Upgrading biomass-derived pyrolysis bio-oil to bio-jet fuel through catalytic cracking and hydrodeoxygenation: A review of recent progress. Energy Convers Manag 2022;268:115956.
[7] D.-C. Lv, K. Jiang, K. Li, Y.-Q. Liu, D. Wang, Y.-Y. Ye, Effective suppression of coke formation with lignin-derived oil during the upgrading of pyrolysis oils, Biomass and Bioenergy 159 (2022) 106425. https://doi.org/Doi: 10.1016/j.biombioe.2022.106425.
[8] Hilten RN, Das KC. Comparison of three accelerated aging procedures to assess bio-oil stability. Fuel 2010;89:2741–9.
[9] Janosik T, Nilsson AN, Hällgren A-C, Hedberg M, Bernlind C, Rådberg H, et al. Derivatizing of fast pyrolysis bio-oil and coprocessing in fixed bed hydrotreater. Energy Fuel 2022;36:8274–87. https://doi.org/10.1021/acs.energyfuels.2c01608.
[10] Gong S, Shinozaki A, Shi M, Qian EW. Hydrotreating of jatropha oil over alumina based catalysts. Energy Fuel 2012;26:2394–9. https://doi.org/10.1021/ef300047a.
[11] Grilc M, Likozar B, Levec J. Simultaneous liquefaction and hydrodeoxygenation of lignocellulosic biomass over NiMo/Al2O3, Pd/Al2O3, and zeolite Y catalysts in hydrogen donor solvents. ChemCatChem 2016;8:180–91. https://doi.org/10.1002/cctc.201500840.
[12] Hu X, Zhang Z, Gholizadeh M, Zhang S, Lam CH, Xiong Z, et al. Coke formation during thermal treatment of bio-oil. Energy Fuel 2020;34:7863–914. https://doi.org/10.1021/acs.energyfuels.0c01323.
[13] Yan P, Mensah J, Drewery M, Kennedy E, Maschmeyer T, Stockenhuber M. Role of metal support during ru-catalysed hydrodeoxygenation of biocrude oil. Appl Catal B Environ 2021;281:119470. https://doi.org/10.1016/j.apcatb.2020.119470.
[14] Djandja OS, Wang Z, Duan P, Wang F, Xu Y. Hydrotreatment of pyrolysis oil from waste tire in tetralin for production of high-quality hydrocarbon rich fuel. Fuel 2021;285:119185. https://doi.org/10.1016/j.fuel.2020.119185.
[15] Han Y, Gholizadeh M, Tran CC, Kaliaguine S, Li CZ, Olarte M, et al. Hydrotreatment of pyrolysis bio-oil: A review. Fuel Process Technol 2019;195:106140.
[16] Dabros TMH, Stummann MZ, Høj M, Jensen PA, Grunwaldt J-D, Gabrielsen J, et al. Transportation fuels from biomass fast pyrolysis, catalytic hydrodeoxygenation, and catalytic fast hydropyrolysis. Prog Energy Combust Sci 2018;68:268.
[17] Kim G, Seo J, Choi J-W, Jae J, Ha J-M, Suh DJ, et al. Two-step continuous upgrading of sawdust pyrolysis oil to deoxygenated hydrocarbons using hydrotreating and hydrodeoxygenating catalysts. Catal Today 2018;303:130–5.
[18] Yin W, Wang Z, Yang H, Venderbosch RH, Heeres HJ. Catalytic hydrotreatment of biomass-derived fast pyrolysis liquids using Ni and Cu-based PRICAT catalysts. Energy Fuel 2022.
[19] Cheng S, Wei L, Julson J, Rabnawaz M. Upgrading pyrolysis bio-oil through hydrodeoxygenation (HDO) using non-sulfided Fe-Co/SiO2 catalyst. Energy Convers Manag 2017;150:331–42.
[20] Priharto N, Ronsse F, Prins W, Carleer R, Heeres HJ. Experimental studies on a two-step fast pyrolysis-catalytic hydrotreatment process for hydrocarbons from microalgae (Nannochloropsis gaditana and Scenedesmus almeriensis). Fuel Process Technol 2020;206:106466. https://doi.org/10.1016/j.fuproc.2020.106466.
[21] Yin W, Gu H, Figueirêdo MB, Xia S, Venderbosch RH, Heeres HJ. Stabilization of fast pyrolysis liquids from biomass by catalytic hydrotreatment using Raney nickel

"type" catalysts. Fuel Process Technol 2021;219:106846. https://doi.org/10.1016/j.fuproc.2021.106846.
[22] Venderbosch RH, Ardiyanti AR, Wildschut J, Oasmaa A, Heeres HJ. Stabilization of biomass-derived pyrolysis oils. J Chem Technol Biotechnol 2010;85:674–86.
[23] Meng J, Moore A, Tilotta DC, Kelley SS, Adhikari S, Park S, et al. Energy Fuel 2015;29:5117–26.
[24] Black S, Ferrell JR. Accelerated aging of fast pyrolysis bio-oil: a new method based on carbonyl titration. RSC Adv 2020;10:10046–54.
[25] Wang R, Ben H. Accelerated aging process of bio-oil model compounds: a mechanism study. Front Energy Res 2020;8:79.
[26] Payormhorm J, Kangvansaichol K, Reubroycharoen P, Kuchonthara P, Hinchiranan N. Pt/Al2O3-catalytic deoxygenation for upgrading of Leucaena leucocephala-pyrolysis oil. Bioresour Technol 2013;139:128.
[27] Wildschut J, Mahfud FH, Venderbosch RH, Heeres HJ. Hydrotreatment of fast pyrolysis oil using heterogeneous noble-metal catalysts. Ind Eng Chem Res 2009;48:10324.
[28] Lee CR, Yoon JS, Suh Y-W, Choi J-W, Ha J-M, Suh DJ, et al. Park, Catalytic roles of metals and supports on hydrodeoxygenation of lignin monomer guaiacol. Catal Commun 2012;17:54–8. https://doi.org/10.1016/j.catcom.2011.10.011.
[29] He Z, Wang X. Highly selective catalytic hydrodeoxygenation of guaiacol to cyclohexane over Pt/TiO2 and NiMo/Al2O3 catalysts. Front Chem Sci Eng 2014;8:369–77. https://doi.org/10.1007/s11705-014-1435-9.
[30] Nimmanwudipong T, Runnebaum RC, Tay K, Block DE, Gates BC. Cyclohexanone conversion catalyzed by Pt/γ-Al2O3: Evidence of oxygen removal and coupling reactions. Catal Lett 2011;141:1072–8. https://doi.org/10.1007/s10562-011-0659-2.
[31] S. Bhogeswararao, D. Srinivas, Catalytic conversion of furfural to industrial chemicals over supported Pt and Pd catalysts, J. Catal. 327 (2015) 65–77. https://doi.org/Doi: 10.1016/j.jcat.2015.04.018.
[32] J. Lee, Y. Xu, G.W. Huber, High-throughput screening of monometallic catalysts for aqueous-phase hydrogenation of biomass-derived oxygenates, Appl. Catal. B Environ. 140–141 (2013) 98–107. https://doi.org/Doi: 10.1016/j.apcatb.2013.03.031.
[33] Zanuttini MS, Peralta MA, Querini CA. Deoxygenation of m-cresol: Deactivation and regeneration of Pt/γ-Al2O3 catalysts. Ind Eng Chem Res 2015;54:4929–39.
[34] Shumeiko B, Schlackl K, Kubička D. Hydrogenation of bio-oil model compounds over Raney-Ni at ambient pressure. Catalysts 2019;9:268.
[35] Xu Y, Long J, Liu Q, Li Y, Wang C, Zhang Q, et al. In situ hydrogenation of model compounds and raw bio-oil over Raney Ni catalyst. Energy Convers Manag 2015;89:188–96.
[36] Wan H, Chaudhari RV, Subramaniam B. Aqueous phase hydrogenation of acetic acid and its promotional effect on *p* -cresol hydrodeoxygenation. Energy Fuel 2013;27:487–93. https://doi.org/10.1021/ef301400c.
[37] Chen J, Wang S, Lu L, Zhang X, Liu Y. Improved catalytic upgrading of simulated bio-oil via mild hydrogenation over bimetallic catalysts. Fuel Process Technol 2018;179:135–42. https://doi.org/10.1016/j.fuproc.2018.06.022.
[38] Han D, Yin W, Arslan A, Liu T, Zheng Y, Xia S. Stabilization of fast pyrolysis liquids from biomass by mild catalytic hydrotreatment: Model compound study. Catalysts 2020;10:402. https://doi.org/10.3390/catal10040402.
[39] Boscagli C, Raffelt K, Zevaco TA, Olbrich W, Otto TN, Sauer J, et al. Mild hydrotreatment of the light fraction of fast-pyrolysis oil produced from straw over nickel-based catalysts. Biomass Bioenergy 2015;83:525–38.
[40] Xu Y, Li Y, Wang C, Wang C, Ma L, Wang T, et al. In-situ hydrogenation of model compounds and raw bio-oil over Ni/CMK-3 catalyst. Fuel Process Technol 2017;161:226–31.
[41] Guo J, Ruan R, Zhang Y. Hydrotreating of phenolic compounds separated from bio-oil to alcohols. Ind Eng Chem Res 2012;51:6599–604.
[42] Xu Y, Zhang L, Chang J, Zhang X, Ma L, Wang T, et al. One step hydrogenation–esterification of model compounds and bio-oil to alcohols and esters over Raney Ni catalysts. Energy Convers Manag 2016;108:78–84.
[43] Nejadmoghadam E, Achour A, Sirous-Rezaei P, Salam MA, Arora P, Öhrman O, et al. Stabilization of bio-oil from simulated pyrolysis oil using sulfided NiMo/Al2O3 catalyst. Fuel 2023;353:129094.
[44] Sun K, Zhang L, Xu Q, Zhang Z, Shao Y, Dong D, et al. Evidence for cross-polymerization between the biomass-derived furans and phenolics. Renew Energy 2020;154:517–31. https://doi.org/10.1016/j.renene.2020.03.030.
[45] Xu Q, Sun K, Shao Y, Zhang C, Zhang S, Zhang L, et al. Cross-polymerisation between furfural and the phenolics of varied molecular structure in bio-oil. Bioresour Technol Reports 2019;8:100324. https://doi.org/10.1016/j.biteb.2019.100324.
[46] Xu Q, Zhang L, Sun K, Shao Y, Tian H, Zhang S, et al. Cross-polymerisation between the model furans and carbohydrates in bio-oil with acid or alkaline catalysts. J Energy Inst 2020;93:1678–89. https://doi.org/10.1016/j.joei.2020.02.005.
[47] Barroso-Martín I, Ballesteros-Plata D, Infantes-Molina A, Guerrero-Pérez MO, Santamaría-González J, Rodríguez-Castellón E. An overview of catalysts for the hydrodeoxygenation reaction of model compounds from lignocellulosic biomass. IET Renew Power Gener 2022;16:3009–22.
[48] Rao TU, Suchada S, Choi C, Machida H, Huo Z, Norinaga K. Selective hydrogenation of furfural to tetrahydrofurfuryl alcohol in 2-butanol over an equimolar Ni-Cu-Al catalyst prepared by the co-precipitation method. Energy Convers Manag 2022;265:115736.
[49] Ouedraogo AS, Bhoi PR. Recent progress of metals supported catalysts for hydrodeoxygenation of biomass derived pyrolysis oil. J Clean Prod 2020;253:119957.
[50] Kim H, Lee J, Kim Y, Ha J-M, Park Y-K, Vlachos DG, et al. Chem Eng J 2024;481:148328.
[51] Xu X, Li Y, Gong Y, Zhang P, Li H, Wang Y. Synthesis of palladium nanoparticles supported on mesoporous N-doped carbon and their catalytic ability for biofuel upgrade. J Am Chem Soc 2012;134:16987–90.
[52] N. Tran, Y. Uemura, T. Trinh, A. Ramli, Hydrodeoxygenation of Guaiacol over Pd–Co and Pd–Fe Catalysts: Deactivation and Regeneration. Processes 2021, 9, 430, Met. Nanoparticles as Catal. Green Appl. (2021) 5.
[53] Zanuttini MS, Dalla Costa BO, Querini CA, Peralta MA. Hydrodeoxygenation of m-cresol with Pt supported over mild acid materials. Appl Catal A Gen 2014;482:352–61.
[54] He Y, Liu R, Yellezuome D, Peng W, Tabatabaei M. Upgrading of biomass-derived bio-oil via catalytic hydrogenation with Rh and Pd catalysts. Renew Energy 2022;184:487–97.
[55] Okoroigwe EC, Li Z, Kelkar S, Saffron C, Onyegegbu S. Bio-oil yield potential of some tropical woody biomass. J Energy South Africa 2015;26:33–41.
[56] M. Asadieraghi, W.M. Ashri Wan Daud, H.F. Abbas, Heterogeneous catalysts for advanced bio-fuel production through catalytic biomass pyrolysis vapor upgrading: a review, RSC Adv. 5 (2015) 22234–22255. Doi: 10.1039/C5RA00762C.
[57] Liu C, Wang H, Karim AM, Sun J, Wang Y. Catalytic fast pyrolysis of lignocellulosic biomass. Chem Soc Rev 2014;43:7594–623.
[58] Olsson Månsson E, Achour A, Ho PH, Arora P, Öhrman O, Creaser D, et al. Removal of inorganic impurities in the fast pyrolysis bio-oil using sorbents at ambient temperature. Energy Fuel 2023;38:414–25.
[59] Muangsuwan C, Kriprasertkul W, Ratchahat S, Liu C-G, Posoknistakul P, Laosiripojana N, et al. Upgrading of light bio-oil from solvothermolysis liquefaction of an oil palm empty fruit bunch in glycerol by catalytic hydrodeoxygenation using NiMo/Al2O3 or CoMo/Al2O3 catalysts. ACS Omega 2021;6:2999–3016. https://doi.org/10.1021/acsomega.0c05387.
[60] Abdus Salam M, Wayne Cheah Y, Hoang Ho P, Bernin D, Achour A, Nejadmoghadam E, et al. Elucidating the role of NiMoS-USY during the hydrotreatment of Kraft lignin. Chem Eng J 2022;442. https://doi.org/10.1016/j.cej.2022.136216.
[61] Garidzirai R, Modisha P, Shuro I, Visagie J, van Helden P, Bessarabov D. The effect of Mg and Zn dopants on Pt/Al2O3 for the dehydrogenation of perhydrodibenzyltoluene. Catalysts 2021;11. https://doi.org/10.3390/catal11040490.
[62] Teles CA, Rabelo-Neto RC, de Lima JR, Mattos LV, Resasco DE, Noronha FB. The effect of metal type on hydrodeoxygenation of phenol over silica supported catalysts. Catal Letters 2016;146:1848–57. https://doi.org/10.1007/s10562-016-1815-5.
[63] Dabros TMH, Andersen ML, Lindahl SB, Hansen TW, Høj M, Gabrielsen J, et al. Hydrodeoxygenation (HDO) of aliphatic oxygenates and phenol over NiMo/MgAl2O4: Reactivity, inhibition, and catalyst reactivation. Catalysts 2019;9:521.
[64] Wildschut J, Arentz J, Rasrendra CB, Venderbosch RH, Heeres HJ. Catalytic hydrotreatment of fast pyrolysis oil: Model studies on reaction pathways for the carbohydrate fraction. Environ Prog Sustain Energy 2009;28:450–60. https://doi.org/10.1002/ep.10390.
[65] Akwasi A.Boateng, Pyrolysis of Biomass for Fuels and Chemicals, 2020.
[66] Pujro R, García JR, Bertero M, Falco M, Sedran U. Review on reaction pathways in the catalytic upgrading of biomass pyrolysis liquids. Energy Fuel 2021;35:16943–64. https://doi.org/10.1021/acs.energyfuels.1c01931.
[67] Stöcker M, Weitkamp J. Catalysis: Methanol to hydrocarbons. Micropor Mesopor Mater 1999;29.
[68] S. Oh, H. Hwang, H.S. Choi, J.W. Choi, The effects of noble metal catalysts on the bio-oil quality during the hydrodeoxygenative upgrading process, Fuel 153 (2015) 535–543. https://doi.org/Doi: 10.1016/j.fuel.2015.03.030.
[69] Li Y, Zhang C, Liu Y, Tang S, Chen G, Zhang R, et al. Coke formation on the surface of Ni/HZSM-5 and Ni-Cu/HZSM-5 catalysts during bio-oil hydrodeoxygenation. Fuel 2017;189:23–31. https://doi.org/10.1016/j.fuel.2016.10.047.
[70] Hu X, Nango K, Bao L, Li T, Hasan MDM, Li C-Z. High yields of solid carbonaceous materials from biomass. Green Chem 2019;21:1128–40. https://doi.org/10.1039/C8GC03153C.
[71] Wiesfeld JJ, Kim M, Nakajima K, Hensen EJM. Selective hydrogenation of 5-hydroxymethylfurfural and its acetal with 1,3-propanediol to 2,5-bis(hydroxymethyl)furan using supported rhenium-promoted nickel catalysts in water. Green Chem 2020;22:1229–38. https://doi.org/10.1039/C9GC03856F.
[72] Hu X, Li C-Z. Levulinic esters from the acid-catalysed reactions of sugars and alcohols as part of a bio-refinery. Green Chem 2011;13:1676. https://doi.org/10.1039/c1gc15272f.
[73] Chuntanapum A, Matsumura Y. Char formation mechanism in supercritical water gasification process: A study of model compounds. Ind Eng Chem Res 2010;49:4055–62. https://doi.org/10.1021/ie901346h.
[74] French RJ, Stunkel J, Black S, Myers M, Yung MM, Iisa K. Evaluate impact of catalyst type on oil yield and hydrogen consumption from mild hydrotreating. Energy Fuel 2014;28:3086–95. https://doi.org/10.1021/ef4019349.
[75] Eschenbacher A, Saraeian A, Shanks BH, Jensen PA, Li C, Duus JØ, et al. Enhancing bio-oil quality and energy recovery by atmospheric hydrodeoxygenation of wheat straw pyrolysis vapors using Pt and Mo-based catalysts. Sustain Energy Fuels 2020;4:1991–2008.
[76] Zhang W, Zhang Y, Zhao L, Wei W. Catalytic activities of NiMo carbide supported on SiO2 for the hydrodeoxygenation of ethyl benzoate, acetone, and acetaldehyde. Energy Fuel 2010;24:2052–9. https://doi.org/10.1021/ef901222z.
[77] D.W. Ball, J.W. Hill, R.J. Scott, chapter 14, in: TThe Basics Gen. Org. Biol. Chem. Saylor, 2011.
[78] Boscagli C, Raffelt K, Grunwaldt J-D. Reactivity of platform molecules in pyrolysis oil and in water during hydrotreatment over nickel and ruthenium catalysts. Biomass Bioenergy 2017;106:63.

[79] Smirnov AA, Alekseeva MV, Bulavchenko OA, Yakovlev VA. Studying the effect of the process temperature on the degree of bio-oil hydrotreatment at low hydrogen contents over NiCu–SiO 2 catalyst with a high metal loading. Catal Ind 2019;11:65–73.
[80] Achour A, Bernin D, Creaser D, Olsson L. Evaluation of kraft and hydrolysis lignin hydroconversion over unsupported NiMoS catalyst. Chem Eng J 2023;453:139829.
[81] Hao N, Ben H, Yoo CG, Adhikari S, Ragauskas AJ. Review of NMR characterization of pyrolysis oils. Energy Fuel 2016;30:6863–80.
[82] Ferrell III JR, Olarte MV, Christensen ED, Padmaperuma AB, Connatser RM, Stankovikj F, et al. Standardization of chemical analytical techniques for pyrolysis bio-oil: history, challenges, and current status of methods. Biofuels Bioprod Biorefining 2016;10:496–507.
[83] Meng X, Crestini C, Ben H, Hao N, Pu Y, Ragauskas AJ, et al. Determination of hydroxyl groups in biorefinery resources via quantitative 31P NMR spectroscopy. Nat Protoc 2019;14:2627–47.
[84] M. V Olarte, S.D. Burton, M. Swita, A.B. Padmaperuma, J. Ferrell, H. Ben, Determination of Hydroxyl Groups in BIOREFIN, National Renewable Energy Lab. (NREL), Golden, CO (United States), 2016.
[85] Gunawan R, Li X, Larcher A, Hu X, Mourant D, Chaiwat W, et al. Hydrolysis and glycosidation of sugars during the esterification of fast pyrolysis bio-oil. Fuel 2012;95:146–51. https://doi.org/10.1016/j.fuel.2011.08.032.
[86] Bengoechea MO, Hertzberg A, Miletić N, Arias PL, Barth T. Simultaneous catalytic de-polymerization and hydrodeoxygenation of lignin in water/formic acid media with Rh/Al2O3, Ru/Al2O3 and Pd/Al2O3 as bifunctional catalysts. J Anal Appl Pyrolysis 2015;113:713–22.
[87] Yu Y, Chua YW, Wu H. Characterization of pyrolytic sugars in bio-oil produced from biomass fast pyrolysis. Energy Fuel 2016;30:4145–9. https://doi.org/10.1021/acs.energyfuels.6b00464.
[88] Cai J, Rahman MM, Zhang S, Sarker M, Zhang X, Zhang Y, et al. Review on aging of bio-oil from biomass pyrolysis and strategy to slowing aging. Energy Fuel 2021;35:11665–92.
[89] M.E. Boucher, A. Chaala, H. Pakdel, C. Roy, Bio-oils obtained by vacuum pyrolysis of softwood bark as a liquid fuel for gas turbines. Part II: Stability and ageing of bio-oil and its blends with methanol and a pyrolytic aqueous phase, Biomass and Bioenergy 19 (2000) 351–361.
[90] J.P. Diebold, A Review of the Chemical and Physical Mechanisms of the Storage Stability of Fast Pyrolysis Bio-Oils, 1999.
[91] Patil SKR, Lund CRF. Formation and growth of humins via aldol addition and condensation during acid-catalyzed conversion of 5-hydroxymethylfurfural. Energy Fuel 2011;25:4745–55.
[92] Ben H, Ferrell III JR. In-depth investigation on quantitative characterization of pyrolysis oil by 31 P NMR. RSC Adv 2016;6:17567–73.
[93] Kaur J, Sarma AK, Gera P, Jha MK. Process optimization with acid functionalised activated carbon derived from corncob for production of 4-hydroxymethyl-2, 2-dimethyl-1, 3-dioxolane and 5-hydroxy-2, 2-dimethyl-1, 3-dioxane. Sci Rep 2021;11:1–12.
[94] Li Z, Jiang E, Xu X, Sun Y, Tu R. Hydrodeoxygenation of phenols, acids, and ketones as model bio-oil for hydrocarbon fuel over Ni-based catalysts modified by Al, La and Ga. Renew Energy 2020;146:1991–2007.
[95] S.F. Zaman, H.S. Bamufleh, A. Al-Zahrani, M.R.A. Rafiqui, Y.A. Alhamed, L. Petrov, Acetic acid hydrogenation over silica supported mop catalyst, Compt. Rend. Acad. Bulg. Sci. 71 (n.d.) 2018.
[96] Wang H, Lee S-J, Olarte MV, Zacher AH. Bio-oil stabilization by hydrogenation over reduced metal catalysts at low temperatures. ACS Sustain Chem Eng 2016;4:5533.
[97] Lazaridis PA, Karakoulia S, Delimitis A, Coman SM, Parvulescu VI, Triantafyllidis KS. D-Glucose hydrogenation/hydrogenolysis reactions on noble metal (Ru, Pt)/activated carbon supported catalysts. Catal Today 2015;257:281–90.